

Semileptonic D Meson Decays $D \rightarrow P/V/S\ell^+\nu_\ell$ with the SU(3) Flavor Symmetry/Breaking

Ru-Min Wang^{1,†}, Yue-Xin Liu¹, Chong Hua¹, Jin-Huan Sheng^{2,§}, Yuan-Guo Xu^{1,‡}

¹College of Physics and Communication Electronics, Jiangxi Normal University, Nanchang, Jiangxi 330022, China

²School of Physics and Engineering, Henan University of Science and Technology, Luoyang, Henan 471000, China

[†]ruminwang@sina.com [§]jinhuanwuli@126.com [‡]yuanguoxu@jxnu.edu.cn

Many exclusive $c \rightarrow d/s\ell^+\nu_\ell$ ($\ell = e, \mu, \tau$) transitions have been well measured, and they can be used to test the theoretical calculations. Motivated by this, we study the $D \rightarrow P/V/S\ell^+\nu_\ell$ decays induced by the $c \rightarrow d/s\ell^+\nu_\ell$ transitions with the SU(3) flavor symmetry approach, where P denotes the pseudoscalar meson, V denotes the vector meson, and S denotes the scalar meson with a mass below 1 GeV. The different decay amplitudes of the $D \rightarrow P\ell^+\nu_\ell$, $D \rightarrow V\ell^+\nu_\ell$ or $D \rightarrow S\ell^+\nu_\ell$ decays can be related by using the SU(3) flavor symmetry and by considering the SU(3) flavor breaking. Using the present data of $D \rightarrow P/V/S\ell^+\nu_\ell$, we predict the not yet measured or not yet well measured processes in the $D \rightarrow P/V/S\ell^+\nu_\ell$ decays. We find that the SU(3) flavor symmetry approach works well in the semileptonic $D \rightarrow P/V\ell^+\nu_\ell$ decays. For the $D \rightarrow S\ell^+\nu_\ell$ decays, only the decay $D_s^+ \rightarrow f_0(980)e^+\nu_e$ has been measured, the branching ratios of the $D_s^+ \rightarrow f_0(980)e^+\nu_e$ and $D \rightarrow S(S \rightarrow P_1P_2)\ell^+\nu_\ell$ decays are used to constrain the nonperturbative parameters and then predict not yet measured $D \rightarrow S\ell^+\nu_\ell$ decays, in addition, the two quark and the four quark scenarios for the light scalar mesons are analyzed. The SU(3) flavor symmetry predictions of the $D \rightarrow S\ell^+\nu_\ell$ decays need to be further tested, and our predictions of the $D \rightarrow S\ell^+\nu_\ell$ decays are useful for probing the structure of light scalar mesons. Our results in this work could be used to test the SU(3) flavor symmetry approach in the semileptonic D decays by the future experiments at BESIII, LHCb and BelleII.

I. Introduction

Semileptonic heavy meson decays dominated by tree-level exchange of W -bosons in the standard model have attracted a lot of attention in testing the stand model and in searching for the new physics beyond the stand model. Many semileptonic $D \rightarrow P/V\ell^+\nu_\ell$ decays and one $D \rightarrow S\ell^+\nu_\ell$ decay have been observed [1], and present experimental measurements give us an opportunity to additionally test theoretical approaches.

In theory, the description of semileptonic decays are relatively simple, and the weak and strong dynamics can be separated in these processes since leptons do not participate in the strong interaction. All the strong dynamics in the initial and final hadrons is included in the hadronic form factors, which are important for testing the theoretical calculations of the involved strong interaction. The form factors of the D decays have been calculated, for examples, by quark model [2–7], QCD sum rules [8], light-cone sum rules [9–11], covariant light-front quark models [12–14], and lattice QCD [15, 16].

The SU(3) flavor symmetry approach is independent of the detailed dynamics offering us an opportunity to relate different decay modes, nevertheless, it cannot determine the sizes of the amplitudes or the form factors by itself.

However, if experimental data are enough, one may use the data to extract the amplitudes or the form factors, which can be viewed as predictions based on symmetry, has a smaller dependency on estimated form factors, and can provide some very useful information about the decays. The SU(3) flavor symmetry works well in the b -hadron decays [17–30], and the c -hadron decays [29–45].

Semileptonic decays of D mesons have been studied extensively in the standard model and its various extensions, for instance, in Refs. [3, 46–56]. In this work, we will systematically study the $D \rightarrow P/V/S\ell^+\nu_\ell$ decays with the SU(3) flavor symmetry. We will firstly construct the amplitude relations between different decay modes of $D \rightarrow P\ell^+\nu_\ell$, $D \rightarrow V\ell^+\nu_\ell$ or $D \rightarrow S\ell^+\nu_\ell$ decays by the SU(3) flavor symmetry and the SU(3) flavor breaking. We use the available data to extract the SU(3) flavor symmetry/breaking amplitudes and the form factors, and then predict the not yet measured modes for further tests in experiments. The forward-backward asymmetries A_{FB}^ℓ , the lepton-side convexity parameters C_F^ℓ , the longitudinal polarizations of the final charged lepton P_L^ℓ , the transverse polarizations of the final charged lepton P_T^ℓ , the lepton spin asymmetries A_λ and the longitudinal polarization fractions F_L of the final vector mesons with two ways of integration have also been predicted in the $D \rightarrow P/V\ell^+\nu_\ell$ decays. In addition, the q^2 dependence of some differential observables for the $D \rightarrow P/V\ell^+\nu_\ell$ decays are shown in figures.

This paper will be organized as follows. In Sec. II, the theoretical framework in this work is presented, including the effective hamiltonian, the hadronic helicity amplitude relations, the observables and the form factors. The numerical results of the $D \rightarrow P/V/S\ell^+\nu_\ell$ semileptonic decays will be given in Sec. III. Finally, we give the summary and conclusion in Sec. IV.

II. Theoretical Frame

A. The effective Hamiltonian

In the standard model, the four-fermion charged-current effective Hamiltonian below the electroweak scale for the decays $D \rightarrow M\ell^+\nu_\ell$ ($M = P, V, S$) can be written as

$$\mathcal{H}_{eff}(c \rightarrow q\ell^+\nu_\ell) = \frac{G_F}{\sqrt{2}} V_{cq}^* \bar{q}\gamma^\mu(1 - \gamma_5)c \bar{\nu}_\ell\gamma_\mu(1 - \gamma_5)\ell, \quad (1)$$

with $q = s, d$.

The helicity amplitudes of the decays $D \rightarrow M\ell^+\nu_\ell$ can be written as

$$\mathcal{M}(D \rightarrow M\ell^+\nu_\ell) = \frac{G_F}{\sqrt{2}} V_{cb} \sum_{mm'} g_{mm'} L_m^{\lambda_\ell\lambda_\nu} H_{m'}^{\lambda_M}, \quad (2)$$

with

$$L_m^{\lambda_\ell\lambda_\nu} = \epsilon_\alpha(m) \bar{\nu}_\ell \gamma^\alpha (1 - \gamma_5) \ell, \quad (3)$$

$$H_{m'}^{\lambda_M} = \begin{cases} \epsilon_\beta^*(m') \langle P/S(p_{P/S}) | \bar{q} \gamma^\beta (1 - \gamma_5) c | D(p_D) \rangle \\ \epsilon_\beta^*(m') \langle V(p_V, \epsilon^*) | \bar{q} \gamma^\beta (1 - \gamma_5) c | D(p_D) \rangle \end{cases}, \quad (4)$$

where the particle helicities $\lambda_M = 0$ for $M = P/S$, $\lambda_M = 0, \pm 1$ for $M = V$, $\lambda_\ell = \pm \frac{1}{2}$ and $\lambda_\nu = +\frac{1}{2}$, as well as $\epsilon_\mu(m)$ is the polarization vectors of the virtual W with $m = 0, t, \pm 1$.

The form factors of the $D \rightarrow P$, $D \rightarrow S$ and $D \rightarrow V$ transitions are given by [2, 3, 13]

$$\langle P(p) | \bar{d}_k \gamma_\mu c | D(p_D) \rangle = f_+^P(q^2)(p + p_D)_\mu + [f_0^P(q^2) - f_+^P(q^2)] \frac{m_D^2 - m_P^2}{q^2} q_\mu, \quad (5)$$

$$\langle S(p) | \bar{d}_k \gamma_\mu \gamma_5 c | D(p_D) \rangle = -i \left(f_+^S(q^2)(p + p_D)_\mu + [f_0^S(q^2) - f_+^S(q^2)] \frac{m_D^2 - m_S^2}{q^2} q_\mu \right), \quad (6)$$

$$\begin{aligned} \langle V(p, \varepsilon^*) | \bar{d}_k \gamma_\mu (1 - \gamma_5) c | D(p_D) \rangle &= \frac{2V^V(q^2)}{m_D + m_V} \epsilon_{\mu\nu\alpha\beta} \varepsilon^{*\nu} p_D^\alpha p^\beta \\ &- i \left[\varepsilon_\mu^* (m_D + m_V) A_1^V(q^2) - (p_D + p)_\mu (\varepsilon^* \cdot p_D) \frac{A_2^V(q^2)}{m_D + m_V} \right] \\ &+ i q_\mu (\varepsilon^* \cdot p_D) \frac{2m_V}{q^2} [A_3^V(q^2) - A_0^V(q^2)], \end{aligned} \quad (7)$$

where $s = q^2$ ($q = p_D - p_M$), and ε^* is the polarization of vector meson. The hadronic helicity amplitudes can be written as

$$H_\pm = 0, \quad (8)$$

$$H_0 = \frac{2m_{D_q} |\vec{p}_P|}{\sqrt{q^2}} f_+^P(q^2), \quad (9)$$

$$H_t = \frac{m_{D_q}^2 - m_P^2}{\sqrt{q^2}} f_0^P(q^2), \quad (10)$$

for $D \rightarrow P \ell^+ \nu_\ell$ decays,

$$H_\pm = 0, \quad (11)$$

$$H_0 = \frac{i2m_{D_q} |\vec{p}_S|}{\sqrt{q^2}} f_+^S(q^2), \quad (12)$$

$$H_t = \frac{im_{D_q}^2 - m_S^2}{\sqrt{q^2}} f_0^S(q^2), \quad (13)$$

for $D \rightarrow S \ell^+ \nu_\ell$ decays, and

$$H_\pm = (m_{D_q} + m_V) A_1(q^2) \mp \frac{2m_{D_q} |\vec{p}_V|}{(m_{D_q} + m_V)} V(q^2), \quad (14)$$

$$H_0 = \frac{1}{2m_V \sqrt{q^2}} \left[(m_{D_q}^2 - m_V^2 - q^2)(m_{D_q} + m_V) A_1(q^2) - \frac{4m_{D_q}^2 |\vec{p}_V|^2}{m_{D_q} + m_V} A_2(q^2) \right], \quad (15)$$

$$H_t = \frac{2m_{D_q} |\vec{p}_V|}{\sqrt{q^2}} A_0(q^2), \quad (16)$$

for $D \rightarrow V \ell^+ \nu_\ell$ decays, where $|\vec{p}_M| \equiv \sqrt{\lambda(m_{D_q}^2, m_M^2, q^2)}/2m_{D_q}$ with $\lambda(a, b, c) = a^2 + b^2 + c^2 - 2ab - 2ac - 2bc$.

B. Hadronic helicity amplitude relations by the SU(3) flavor symmetry

Charmed mesons containing one heavy c quark are flavor SU(3) anti-triplets

$$D_i = \left(D^0(c\bar{u}), D^+(c\bar{d}), D_s^+(c\bar{s}) \right). \quad (17)$$

Light pseudoscalar P and vector V meson octets and singlets under the $SU(3)$ flavor symmetry of u, d, s quarks are [57]

$$P = \begin{pmatrix} \frac{\pi^0}{\sqrt{2}} + \frac{\eta_8}{\sqrt{6}} + \frac{\eta_1}{\sqrt{3}} & \pi^+ & K^+ \\ \pi^- & -\frac{\pi^0}{\sqrt{2}} + \frac{\eta_8}{\sqrt{6}} + \frac{\eta_1}{\sqrt{3}} & K^0 \\ K^- & \bar{K}^0 & -\frac{2\eta_8}{\sqrt{6}} + \frac{\eta_1}{\sqrt{3}} \end{pmatrix}, \quad (18)$$

$$V = \begin{pmatrix} \frac{\rho^0}{\sqrt{2}} + \frac{\omega_8}{\sqrt{6}} + \frac{\omega_1}{\sqrt{3}} & \rho^+ & K^{*+} \\ \rho^- & -\frac{\rho^0}{\sqrt{2}} + \frac{\omega_8}{\sqrt{6}} + \frac{\omega_1}{\sqrt{3}} & K^{*0} \\ K^{*-} & \bar{K}^{*0} & -\frac{2\omega_8}{\sqrt{6}} + \frac{\omega_1}{\sqrt{3}} \end{pmatrix}, \quad (19)$$

where ω and ϕ mix in an ideal form, and the η and η' (ω and ϕ) are mixtures of $\eta_1(\omega_1) = \frac{u\bar{u}+d\bar{d}+s\bar{s}}{\sqrt{3}}$ and $\eta_8(\omega_8) = \frac{u\bar{u}+d\bar{d}-2s\bar{s}}{\sqrt{6}}$ with the mixing angle θ_P (θ_V). η and η' (ω and ϕ) are given by

$$\begin{pmatrix} \eta \\ \eta' \end{pmatrix} = \begin{pmatrix} \cos\theta_P & -\sin\theta_P \\ \sin\theta_P & \cos\theta_P \end{pmatrix} \begin{pmatrix} \eta_8 \\ \eta_1 \end{pmatrix}, \quad \begin{pmatrix} \phi \\ \omega \end{pmatrix} = \begin{pmatrix} \cos\theta_V & -\sin\theta_V \\ \sin\theta_V & \cos\theta_V \end{pmatrix} \begin{pmatrix} \omega_8 \\ \omega_1 \end{pmatrix}, \quad (20)$$

where $\theta_P = [-20^\circ, -10^\circ]$ and $\theta_V = 36.4^\circ$ from Particle Data Group (PDG) [1] will be used in our numerical analysis.

The structures of the light scalar mesons are not fully understood yet. Many suggestions are discussed, such as ordinary two quark states, four quark states, meson-meson bound states, molecular states, glueball states or hybrid states, for examples, in Refs. [58–66]. In this work, we will consider the two quark and the four quark scenarios for the scalar mesons below or near 1 GeV. In the two quark picture, the light scalar mesons can be written as [67]

$$S = \begin{pmatrix} \frac{a_0^0}{\sqrt{2}} + \frac{\sigma}{\sqrt{2}} & a_0^+ & K_0^+ \\ a_0^- & -\frac{a_0^0}{\sqrt{2}} + \frac{\sigma}{\sqrt{2}} & K_0^0 \\ K_0^- & \bar{K}_0^0 & f_0 \end{pmatrix}. \quad (21)$$

The two isoscalars $f_0(980)$ and $f_0(500)$ are obtained by the mixing of $\sigma = \frac{u\bar{u}+d\bar{d}}{\sqrt{2}}$ and $f_0 = s\bar{s}$

$$\begin{pmatrix} f_0(980) \\ f_0(500) \end{pmatrix} = \begin{pmatrix} \cos\theta_S & \sin\theta_S \\ -\sin\theta_S & \cos\theta_S \end{pmatrix} \begin{pmatrix} f_0 \\ \sigma \end{pmatrix}, \quad (22)$$

where the three possible ranges of the mixing angle, $25^\circ < \theta_S < 40^\circ$, $140^\circ < \theta_S < 165^\circ$ and $-30^\circ < \theta_S < 30^\circ$ [58, 68] will be analyzed in our numerical results. In the four quark picture, the light scalar mesons are given as [1, 69]

$$\begin{aligned} \sigma &= u\bar{u}d\bar{d}, & f_0 &= (u\bar{u} + d\bar{d})s\bar{s}/\sqrt{2}, \\ a_0^0 &= (u\bar{u} - d\bar{d})s\bar{s}/\sqrt{2}, & a_0^+ &= u\bar{d}s\bar{s}, & a_0^- &= d\bar{u}s\bar{s}, \\ K_0^+ &= u\bar{s}d\bar{d}, & K_0^0 &= d\bar{s}u\bar{u}, & \bar{K}_0^0 &= s\bar{d}u\bar{u}, & K_0^+ &= s\bar{u}d\bar{d}, \end{aligned} \quad (23)$$

and the two isoscalars are expressed as

$$\begin{pmatrix} f_0(980) \\ f_0(500) \end{pmatrix} = \begin{pmatrix} \cos\phi_S & \sin\phi_S \\ -\sin\phi_S & \cos\phi_S \end{pmatrix} \begin{pmatrix} f_0 \\ \sigma \end{pmatrix}, \quad (24)$$

where the constrained mixing angle $\phi_S = (174.6_{-3.2}^{+3.4})^\circ$ [59].

In terms of the SU(3) flavor symmetry, meson states and quark operators can be parameterized into SU(3) tensor forms, while the leptonic helicity amplitudes $L_m^{\lambda_\ell, \lambda_\nu}$ are invariant under the SU(3) flavor symmetry. And the hadronic helicity amplitude relations of the $D \rightarrow M\ell^+\nu_\ell$ ($M = P, V, S$) decays can be parameterized as

$$H(D \rightarrow M\ell^+\nu_\ell) = c_0^M D_i M_j^i H^j, \quad (25)$$

where $H^2 \equiv V_{cd}^*$ and $H^3 \equiv V_{cs}^*$ are the CKM matrix elements, and c_0^M are the nonperturbative coefficients of the $D \rightarrow M\ell^+\nu_\ell$ decays under the SU(3) flavor symmetry. Noted that the hadronic helicity amplitudes for the $D \rightarrow S\ell^+\nu_\ell$ decays in Eq. (25) are given in the two quark picture of the light scalar mesons, and ones in the four quark picture of the light scalar mesons will be given later.

The SU(3) flavor breaking effects mainly come from different masses of u , d and s quarks. Following Ref. [70], the SU(3) breaking amplitudes of the $D \rightarrow M\ell^+\nu_\ell$ decays can be give as

$$\Delta H(D \rightarrow M\ell^+\nu_\ell) = c_1^M D_a W_i^a M_j^i H^j + c_2^M D_i M_a^i W_j^a H^j, \quad (26)$$

with

$$W = (W_j^i) = \begin{pmatrix} 1 & 0 & 0 \\ 0 & 1 & 0 \\ 0 & 0 & -2 \end{pmatrix}, \quad (27)$$

where $c_{1,2}^M$ are the nonperturbative SU(3) flavor breaking coefficients.

In the four quark picture of the light scalar mesons, the hadronic helicity amplitudes of the $D \rightarrow S\ell^+\nu_\ell$ decays under the SU(3) flavor symmetry are

$$H(D \rightarrow S\ell^+\nu_\ell)^{4q} = c_0'^S D_i S_{jm}^{im} H^j. \quad (28)$$

And the corresponding SU(3) flavor breaking amplitudes of the $D \rightarrow S\ell^+\nu_\ell$ decays are

$$\Delta H(D \rightarrow S\ell^+\nu_\ell)^{4q} = c_1'^S D_a W_i^a S_{jm}^{im} H^j + c_2'^S D_i S_{am}^{im} W_j^a H^j + c_1'^S D_i S_{ja}^{im} W_m^a H^j. \quad (29)$$

In terms of the SU(3) flavor symmetry, the hadronic helicity amplitude relations for the $D \rightarrow P\ell^+\nu_\ell$, $D \rightarrow V\ell^+\nu_\ell$ and $D \rightarrow S\ell^+\nu_\ell$ decays are summarized in later Tab. I, Tab. IV and Tab. VIII, respectively.

C. Observables for the $D \rightarrow M\ell^+\nu_\ell$ decays

The double differential branching ratios of the $D \rightarrow M\ell^+\nu_\ell$ decays are [56]

$$\begin{aligned} \frac{d\mathcal{B}(D \rightarrow M\ell^+\nu_\ell)}{dq^2 d(\cos \theta)} &= \frac{\tau_D G_F^2 |V_{cq}|^2 \lambda^{1/2} (q^2 - m_\ell^2)^2}{64(2\pi)^3 M_{D(s)}^3 q^2} \left[(1 + \cos^2 \theta) \mathcal{H}_U + 2 \sin^2 \theta \mathcal{H}_L + 2 \cos \theta \mathcal{H}_P \right. \\ &\quad \left. + \frac{m_\ell^2}{q^2} (\sin^2 \theta \mathcal{H}_U + 2 \cos^2 \theta \mathcal{H}_L + 2 \mathcal{H}_S - 4 \cos \theta \mathcal{H}_{SL}) \right], \end{aligned} \quad (30)$$

where $\lambda \equiv \lambda(m_{D_q}^2, m_M^2, q^2)$, $m_\ell^2 \leq q^2 \leq (m_{D_q} - m_M)^2$, and

$$\mathcal{H}_U = |H_+|^2 + |H_-|^2, \quad \mathcal{H}_L = |H_0|^2, \quad \mathcal{H}_P = |H_+|^2 - |H_-|^2, \quad \mathcal{H}_S = |H_t|^2, \quad \mathcal{H}_{SL} = \Re(H_0 H_t^\dagger). \quad (31)$$

The differential branching ratios integrated over $\cos\theta$ are [56]

$$\frac{d\mathcal{B}(D_{(s)} \rightarrow M\ell^+\nu_\ell)}{dq^2} = \frac{\tau_D G_F^2 |V_{cq}|^2 \lambda^{1/2}(q^2 - m_\ell^2)^2}{24(2\pi)^3 M_{D_{(s)}}^3 q^2} \mathcal{H}_{\text{total}}, \quad (32)$$

with

$$\mathcal{H}_{\text{total}} \equiv (\mathcal{H}_U + \mathcal{H}_L) \left(1 + \frac{m_\ell^2}{2q^2}\right) + \frac{3m_\ell^2}{2q^2} \mathcal{H}_S. \quad (33)$$

The lepton flavor universality in $D_{(s)} \rightarrow M\ell^+\nu_\ell$ is defined in a manner identical $R^{\mu/e}$ as

$$R^{\mu/e} = \frac{\int_{q_{\min}}^{q_{\max}} d\mathcal{B}(D_{(s)} \rightarrow M\mu^+\nu_\mu)/dq^2}{\int_{q_{\min}}^{q_{\max}} d\mathcal{B}(D_{(s)} \rightarrow Me^+\nu_e)/dq^2}. \quad (34)$$

The forward-backward asymmetries are defined as [56]

$$A_{FB}^\ell(q^2) = \frac{\int_{-1}^0 d\cos\theta_\ell \frac{d\mathcal{B}(D \rightarrow M\ell\nu)}{dq^2 d\cos\theta_\ell} - \int_0^1 d\cos\theta_\ell \frac{d\mathcal{B}(D \rightarrow M\ell\nu)}{dq^2 d\cos\theta_\ell}}{\int_{-1}^0 d\cos\theta_\ell \frac{d\mathcal{B}(D \rightarrow M\ell\nu)}{dq^2 d\cos\theta_\ell} + \int_0^1 d\cos\theta_\ell \frac{d\mathcal{B}(D \rightarrow M\ell\nu)}{dq^2 d\cos\theta_\ell}} \quad (35)$$

$$= \frac{3}{4} \frac{\mathcal{H}_P - \frac{2m_\ell^2}{q^2} \mathcal{H}_{SL}}{\mathcal{H}_{\text{total}}}. \quad (36)$$

The lepton-side convexity parameters are given by [56]

$$C_F^\ell(q^2) = \frac{3}{4} \left(1 - \frac{m_\ell^2}{q^2}\right) \frac{\mathcal{H}_U - 2\mathcal{H}_L}{\mathcal{H}_{\text{total}}}. \quad (37)$$

The longitudinal polarizations of the final charged lepton ℓ are defined by [56]

$$P_L^\ell(q^2) = \frac{(\mathcal{H}_U + \mathcal{H}_L) \left(1 - \frac{m_\ell^2}{2q^2}\right) - \frac{3m_\ell^2}{2q^2} \mathcal{H}_S}{\mathcal{H}_{\text{total}}}, \quad (38)$$

and its transverse polarizations are

$$P_T^\ell(q^2) = -\frac{3\pi m_\ell}{8\sqrt{q^2}} \frac{\mathcal{H}_P + 2\mathcal{H}_{SL}}{\mathcal{H}_{\text{total}}}. \quad (39)$$

The lepton spin asymmetry in the $\ell - \bar{\nu}_\ell$ center of mass frame is defined by [71–74]

$$A_\lambda(q^2) = \frac{d\mathcal{B}(D \rightarrow M\ell^+\nu_\ell)[\lambda_\ell = -\frac{1}{2}]/dq^2 - d\mathcal{B}(D \rightarrow M\ell^+\nu_\ell)[\lambda_\ell = +\frac{1}{2}]/dq^2}{d\mathcal{B}(D \rightarrow M\ell^+\nu_\ell)[\lambda_\ell = -\frac{1}{2}]/dq^2 + d\mathcal{B}(D \rightarrow M\ell^+\nu_\ell)[\lambda_\ell = +\frac{1}{2}]/dq^2} \quad (40)$$

$$= \frac{\mathcal{H}_{\text{total}} - \frac{6m_\ell^2}{2q^2} \mathcal{H}_S}{\mathcal{H}_{\text{total}}}. \quad (41)$$

For the $D \rightarrow V\ell^+\nu_\ell$ decays, the longitudinal polarization fractions of the final vector mesons are given by [56]

$$F_L(q^2) = \frac{\mathcal{H}_L \left(1 + \frac{m_\ell^2}{2q^2}\right) + \frac{3m_\ell^2}{2q^2} \mathcal{H}_S}{\mathcal{H}_{\text{total}}}, \quad (42)$$

then its transverse polarization fraction $F_T(q^2) = 1 - F_L(q^2)$.

Noted that, for q^2 -integration of $X(q^2) = A_{FB}^\ell, C_F^\ell, P_L^\ell, P_T^\ell, A_\lambda$ and F_L , following Ref. [75], two ways of integration are considered. The normalized q^2 -integrated observables $\langle X \rangle$ are calculated by separately integrating the numerators and denominators with the same q^2 bins. The “naively integrated” observables are obtained by

$$\bar{X} = \frac{1}{q_{\max}^2 - q_{\min}^2} \int_{q_{\min}^2}^{q_{\max}^2} dq^2 X(q^2). \quad (43)$$

D. Form factors

In order to obtain more precise observables, one also need considering the q^2 dependence of the form factors for the $D \rightarrow P\ell^+\nu_\ell$, $D \rightarrow V\ell^+\nu_\ell$ and $D \rightarrow S\ell^+\nu_\ell$ decays. The following cases will be considered in our analysis of $D \rightarrow P/V\ell^+\nu_\ell$ decays.

C_1 : All form factors are treated as constants without the hadronic momentum-transfer q^2 dependence, and different form factors are related by the SU(3) flavor symmetry, *i.e.*, the SU(3) flavor breaking terms such as $c_{1,2}^M$ and $c_{1,2,3}^S$ in later Tabs. I, IV and VIII are ignored.

C_2 : With the SU(3) flavor symmetry, the modified pole model for the q^2 -dependence of $F_i(q^2)$ is used [76]

$$F_i(q^2) = \frac{F_i(0)}{\left(1 - \frac{q^2}{m_{pole}^2}\right) \left(1 - \alpha_i \frac{q^4}{m_{pole}^4}\right)}, \quad (44)$$

where $m_{pole} = m_{D^{*+}}$ for $c \rightarrow d\ell^+\nu_\ell$ transitions and $m_{pole} = m_{D_s^{*+}}$ for $c \rightarrow s\ell^+\nu_\ell$ transitions, and α_i are free parameters and are different for $f_+^P(q^2)$, $f_0^P(q^2)$, $V(q^2)$, $A_1(q^2)$ and $A_2(q^2)$, we will take $\alpha_i \in [-1, 1]$ in our analysis.

C_3 : With the SU(3) flavor symmetry, following Ref. [2]

$$F_i(q^2) = \frac{F_i(0)}{\left(1 - \frac{q^2}{m_{pole}^2}\right) \left(1 - \sigma_{1i} \frac{q^2}{m_{pole}^2} + \sigma_{2i} \frac{q^4}{m_{pole}^4}\right)} \quad \text{for } f_+^P(q^2) \text{ and } V(q^2), \quad (45)$$

$$F_i(q^2) = \frac{F_i(0)}{\left(1 - \sigma_{1i} \frac{q^2}{m_{pole}^2} + \sigma_{2i} \frac{q^4}{m_{pole}^4}\right)} \quad \text{for } f_0^P(q^2), A_1(q^2) \text{ and } A_2(q^2), \quad (46)$$

where $\sigma_{1,2}$ for the $D \rightarrow \pi$ and $D \rightarrow K^*$ transitions from Ref. [2] will be used in our results.

C_4 : Considering the SU(3) flavor breaking terms such as $c_{1,2}^M$ and $c_{1,2,3}^S$ in later Tabs. I, IV and VIII, the form factors in C_3 case are used.

As for the form factors of the $D \rightarrow S\ell^+\nu_\ell$ decays, we find that the vector dominance model [77] and the double pole model [78] give the similar SU(3) flavor symmetry predictions for the branching ratios of the $D \rightarrow S\ell^+\nu_\ell$ decays. The following form factors from the vector dominance model will be used in the numerical results,

$$F_i(q^2) = \frac{F_i(0)}{\left(1 - q^2/m_{pole}^2\right)} \quad \text{for } f_+^S(q^2) \text{ and } f_0^S(q^2). \quad (47)$$

After considering above q^2 dependence, we only need to focus on the $F_i(0)$. Since these form factors $F_i(0)$ also preserve the SU(3) flavor symmetry, the same relations in Tabs. I, IV and VIII will be used for $F_i(0)$. If considering the form factors ratios $f_+(0)/f_0(0) = 1$ for $D \rightarrow P/S\ell^+\nu_\ell$ decays, $r_V \equiv V(0)/A_1(0) = 1.46 \pm 0.07$, $r_2 \equiv A_2(0)/A_1(0) = 0.68 \pm 0.06$ in $D^0 \rightarrow K^{*-}\ell^+\nu_\ell$ decays from PDG [1] and the SU(3) flavor symmetry, there is only one free form factor $f_+^{P,S}(0)$ and $A_1(0)$ for the $D \rightarrow P/S\ell^+\nu_\ell$ and $D \rightarrow V\ell^+\nu_\ell$ decays, respectively. As a result, the branching ratios only depend on one form factor $f_+^P(0)$, $f_+^S(0)$ or $A_1(0)$ and the CKM matrix element V_{cq} .

III. Numerical results

The theoretical input parameters and the experimental data within the 2σ errors from PDG [1] will be used in our numerical results.

A. $D \rightarrow P\ell^+\nu_\ell$ decays

Considering both the SU(3) flavor symmetry and the SU(3) flavor breaking contributions, the hadronic helicity amplitudes for the $D \rightarrow P\ell^+\nu_\ell$ decays are given in Tab. I, in which we keep the CKM matrix element V_{cs} and V_{cd} information for comparing conveniently. In addition, $H(D_s^+ \rightarrow \pi^0\ell^+\nu_\ell)$ are obtained by neutral meson mixing with $\delta^2 = (5.18 \pm 0.71) \times 10^{-4}$ in Ref. [76]. From Tab. I, we can easily see the hadronic helicity amplitude relations of the $D \rightarrow P\ell^+\nu_\ell$ decays. There are four nonperturbative parameters $A_{1,2,3,4}$ in the $D \rightarrow P\ell^+\nu_\ell$ decays with $A_1 \equiv c_0^P + c_1^P - 2c_2^P$, $A_2 \equiv c_0^P - 2c_1^P - 2c_2^P$, $A_3 \equiv c_0^P + c_1^P + c_2^P$ and $A_4 \equiv c_0^P - 2c_1^P + c_2^P$. If neglecting the SU(3) flavor breaking c_1^P and c_2^P terms, $A_1 = A_2 = A_3 = A_4 = c_0^P$, and then all hadronic helicity amplitudes are related by only one parameter c_0^P .

Many decay modes of the $D \rightarrow Pe^+\nu_e, P\mu^+\nu_\mu$ decays have been measured, and the experimental data with 2σ errors are listed in the second column of Tab. II. One can constrain the parameters A_i by the present experimental data within 2σ errors and then predict other not yet measured branching ratios. Four cases $C_{1,2,3,4}$ will be considered in our analysis. The numerical results of $\mathcal{B}(D \rightarrow P\ell^+\nu_\ell)$ in the C_1, C_2, C_3 and C_4 cases are given in the third, forth, fifth and sixth columns of Tab. II, respectively. And our comments on the results are as follows.

- **Results in C_1 case:** From the third column of Tab. II, one can see that the SU(3) flavor symmetry predictions of $\mathcal{B}(D \rightarrow P\ell^+\nu_\ell)$ in the C_1 case are entirely consistent with all present experiential data. The not yet measured branching ratios of the $D_s^+ \rightarrow \pi^0 e^+ \nu_e$, $D_s^+ \rightarrow \pi^0 \mu^+ \nu_\mu$, $D^+ \rightarrow \eta' \mu^+ \nu_\mu$ and $D_s^+ \rightarrow K^0 \mu^+ \nu_\mu$ decays are predicted

TABLE I: The hadronic helicity amplitudes for the $D \rightarrow P\ell^+\nu$ decays including both the SU(3) flavor symmetry and the SU(3) flavor breaking contributions. $A_1 \equiv c_0^P + c_1^P - 2c_2^P$, $A_2 \equiv c_0^P - 2c_1^P - 2c_2^P$, $A_3 \equiv c_0^P + c_1^P + c_2^P$, $A_4 \equiv c_0^P - 2c_1^P + c_2^P$. $A_1 = A_2 = A_3 = A_4 = c_0^P$ if neglecting the SU(3) flavor breaking c_1^P and c_2^P terms.

Hadronic helicity amplitudes	SU(3) flavor amplitudes
$H(D^0 \rightarrow K^-\ell^+\nu_\ell)$	$A_1 V_{cs}^*$
$H(D^+ \rightarrow \bar{K}^0 \ell^+\nu_\ell)$	$A_1 V_{cs}^*$
$H(D_s^+ \rightarrow \eta \ell^+\nu_\ell)$	$(-\cos\theta_P \sqrt{2/3} - \sin\theta_P / \sqrt{3}) A_2 V_{cs}^*$
$H(D_s^+ \rightarrow \eta' \ell^+\nu_\ell)$	$(-\sin\theta_P \sqrt{2/3} + \cos\theta_P / \sqrt{3}) A_2 V_{cs}^*$
$H(D_s^+ \rightarrow \pi^0 \ell^+\nu_\ell)$	$-\delta(-\cos\theta_P \sqrt{2/3} - \sin\theta_P / \sqrt{3}) A_2 V_{cs}^*$
$H(D^0 \rightarrow \pi^-\ell^+\nu_\ell)$	$A_3 V_{cd}^*$
$H(D^+ \rightarrow \pi^0 \ell^+\nu_\ell)$	$-\frac{1}{\sqrt{2}} A_3 V_{cd}^*$
$H(D^+ \rightarrow \eta \ell^+\nu_\ell)$	$(\cos\theta_P / \sqrt{6} - \sin\theta_P / \sqrt{3}) A_3 V_{cd}^*$
$H(D^+ \rightarrow \eta' \ell^+\nu_\ell)$	$(\sin\theta_P / \sqrt{6} + \cos\theta_P / \sqrt{3}) A_3 V_{cd}^*$
$H(D_s^+ \rightarrow K^0 \ell^+\nu_\ell)$	$A_4 V_{cd}^*$

TABLE II: Branching ratios of the $D \rightarrow P\ell^+\nu$ decays. [†]Denotes that the corresponding experimental data from PDG [1] are not used to constrain A_i in this case.

Branching ratios	Exp. data	Ones in C_1	Ones in C_2	Ones in C_3	Ones in C_4	Previous ones
$\mathcal{B}(D^+ \rightarrow \bar{K}^0 e^+ \nu_e)(\times 10^{-2})$	8.72 ± 0.18	8.84 ± 0.06	8.83 ± 0.07	8.84 ± 0.06	8.83 ± 0.07	
$\mathcal{B}(D^+ \rightarrow \pi^0 e^+ \nu_e)(\times 10^{-3})$	3.72 ± 0.34	3.75 ± 0.05	$5.40 \pm 1.33^\dagger$	$5.04 \pm 0.12^\dagger$	3.70 ± 0.11	
$\mathcal{B}(D^+ \rightarrow \eta e^+ \nu_e)(\times 10^{-3})$	1.11 ± 0.14	1.15 ± 0.05	1.20 ± 0.05	1.20 ± 0.05	0.92 ± 0.08	
$\mathcal{B}(D^+ \rightarrow \eta' e^+ \nu_e)(\times 10^{-4})$	2.0 ± 0.8	2.59 ± 0.14	2.22 ± 0.34	2.09 ± 0.14	1.50 ± 0.20	
$\mathcal{B}(D^0 \rightarrow K^- e^+ \nu_e)(\times 10^{-2})$	3.549 ± 0.052	3.52 ± 0.02	3.52 ± 0.03	3.52 ± 0.03	3.52 ± 0.02	
$\mathcal{B}(D^0 \rightarrow \pi^- e^+ \nu_e)(\times 10^{-3})$	2.91 ± 0.08	2.95 ± 0.03	$4.23 \pm 1.03^\dagger$	$3.97 \pm 0.09^\dagger$	2.89 ± 0.06	
$\mathcal{B}(D_s^+ \rightarrow \eta e^+ \nu_e)(\times 10^{-2})$	2.32 ± 0.16	2.37 ± 0.11	2.34 ± 0.14	2.36 ± 0.12	2.32 ± 0.16	
$\mathcal{B}(D_s^+ \rightarrow \eta' e^+ \nu_e)(\times 10^{-3})$	8.0 ± 1.4	9.05 ± 0.04	8.25 ± 1.13	8.04 ± 0.43	8.02 ± 1.38	
$\mathcal{B}(D_s^+ \rightarrow K^0 e^+ \nu_e)(\times 10^{-3})$	3.4 ± 0.8	3.10 ± 0.08	3.56 ± 0.39	3.54 ± 0.12	3.40 ± 0.80	
$\mathcal{B}(D_s^+ \rightarrow \pi^0 e^+ \nu_e)(\times 10^{-5})$	\dots	1.51 ± 0.07	2.10 ± 0.56	1.96 ± 0.10	1.92 ± 0.13	2.65 ± 0.38 [76]
$\mathcal{B}(D^+ \rightarrow \bar{K}^0 \mu^+ \nu_\mu)(\times 10^{-2})$	8.76 ± 0.38	8.56 ± 0.06	8.69 ± 0.15	8.61 ± 0.06	8.61 ± 0.06	
$\mathcal{B}(D^+ \rightarrow \pi^0 \mu^+ \nu_\mu)(\times 10^{-3})$	3.50 ± 0.30	3.67 ± 0.05	$5.32 \pm 1.31^\dagger$	$4.96 \pm 0.12^\dagger$	3.64 ± 0.10	
$\mathcal{B}(D^+ \rightarrow \eta \mu^+ \nu_\mu)(\times 10^{-3})$	1.04 ± 0.22	1.11 ± 0.05	1.18 ± 0.07	1.17 ± 0.05	0.90 ± 0.08	1.21 [7] 0.75 ± 0.15 [79]
$\mathcal{B}(D^+ \rightarrow \eta' \mu^+ \nu_\mu)(\times 10^{-4})$	\dots	2.42 ± 0.13	2.10 ± 0.33	1.96 ± 0.13	1.41 ± 0.19	2.11 [7] 1.06 ± 0.20 [79]
$\mathcal{B}(D^0 \rightarrow K^- \mu^+ \nu_\mu)(\times 10^{-2})$	3.41 ± 0.08	3.41 ± 0.02	3.44 ± 0.05	3.43 ± 0.02	3.43 ± 0.02	
$\mathcal{B}(D^0 \rightarrow \pi^- \mu^+ \nu_\mu)(\times 10^{-3})$	2.67 ± 0.24	2.89 ± 0.02	$4.17 \pm 1.01^\dagger$	$3.90 \pm 0.09^\dagger$	2.85 ± 0.06	
$\mathcal{B}(D_s^+ \rightarrow \eta \mu^+ \nu_\mu)(\times 10^{-2})$	2.4 ± 1.0	2.30 ± 0.10	2.30 ± 0.17	2.31 ± 0.12	2.26 ± 0.16	
$\mathcal{B}(D_s^+ \rightarrow \eta' \mu^+ \nu_\mu)(\times 10^{-2})$	1.1 ± 1.0	0.86 ± 0.03	0.79 ± 0.11	0.77 ± 0.04	0.76 ± 0.13	
$\mathcal{B}(D_s^+ \rightarrow K^0 \mu^+ \nu_\mu)(\times 10^{-3})$	\dots	3.01 ± 0.08	3.51 ± 0.38	3.46 ± 0.11	3.33 ± 0.78	3.9 [7] 3.85 ± 0.76 [79]
$\mathcal{B}(D_s^+ \rightarrow \pi^0 \mu^+ \nu_\mu)(\times 10^{-5})$	\dots	1.48 ± 0.07	2.09 ± 0.53	1.93 ± 0.10	1.89 ± 0.13	
$\mathcal{B}(D_s^+ \rightarrow \pi^0 \tau^+ \nu_\tau)(\times 10^{-10})$	\dots	3.45 ± 0.21	160.34 ± 149.53	4.20 ± 0.26	4.08 ± 0.34	$(27 \sim 36)$ [76]
$R^{\mu/e}(D^+ \rightarrow \bar{K}^0 \ell^+ \nu_\ell)$		0.969	0.984 ± 0.013	0.974	0.974	
$R^{\mu/e}(D^+ \rightarrow \pi^0 \ell^+ \nu_\ell)$		0.977	1.009 ± 0.026	0.984	0.984	
$R^{\mu/e}(D^+ \rightarrow \eta \ell^+ \nu_\ell)$		0.967	0.984 ± 0.014	0.973	0.973	
$R^{\mu/e}(D^+ \rightarrow \eta' \ell^+ \nu_\ell)$		0.935	0.948 ± 0.012	0.940	0.940	
$R^{\mu/e}(D^0 \rightarrow K^- \ell^+ \nu_\ell)$		0.969	0.984 ± 0.013	0.974	0.974	
$R^{\mu/e}(D^0 \rightarrow \pi^- \ell^+ \nu_\ell)$		0.977	1.008 ± 0.026	0.984	0.984	
$R^{\mu/e}(D_s^+ \rightarrow \eta \ell^+ \nu_\ell)$		0.971	0.987 ± 0.013	0.976	0.976	
$R^{\mu/e}(D_s^+ \rightarrow \eta' \ell^+ \nu_\ell)$		0.946	0.958 ± 0.011	0.952	0.952	
$R^{\mu/e}(D_s^+ \rightarrow K^0 \ell^+ \nu_\ell)$		0.973	0.992 ± 0.016	0.978	0.978	
$R^{\mu/e}(D_s^+ \rightarrow \pi^0 \ell^+ \nu_\ell)$		0.980	1.010 ± 0.025	0.985	0.985	

on the order of $\mathcal{O}(10^{-3} - 10^{-5})$, nevertheless, $\mathcal{B}(D_s^+ \rightarrow \pi^0 \tau^+ \nu_\tau)$ is predicted on the order of $\mathcal{O}(10^{-10})$ due to its narrow phase space and $(q^2 - m_\tau^2)^2$ suppression of the differential branching ratios in Eq. (32).

- **Results in $C_{2,3}$ cases:** The numerical results in $C_{2,3}$ cases are similar. The experimental upper limits of $\mathcal{B}(D^+ \rightarrow \pi^0 \ell^+ \nu_\ell)$ and $\mathcal{B}(D^0 \rightarrow \pi^- \ell^+ \nu_\ell)$ have not been used to constrain the predictions of $\mathcal{B}(D \rightarrow P \ell^+ \nu_\ell)$, since the upper limits of the predictions of $\mathcal{B}(D^+ \rightarrow \pi^0 \ell^+ \nu_\ell)$ and $\mathcal{B}(D^0 \rightarrow \pi^- \ell^+ \nu_\ell)$ by the SU(3) flavor symmetry in $C_{2,3}$ cases are slightly larger than their experimental data. Other SU(3) flavor symmetry predictions are consistent with their experimental data within 2σ errors.
- **Results in C_4 case:** As given in the sixth column of Tab. II, if considering both the hadronic momentum-transfer q^2 dependence of the form factors and the SU(3) flavor breaking contributions, all SU(3) flavor symmetry predictions are consistent with their experimental data within 2σ errors. For some decays, the errors of the theoretical predictions are much smaller than ones of their experimental data.
- The previous predictions for the not yet measured branching ratios are listed in the last column of Tab. II, our predictions are in the same order of magnitude as previous ones for the $D \rightarrow P e^+ \nu_e, P \mu^+ \nu_\mu$ decays. And our prediction of $\mathcal{B}(D_s^+ \rightarrow \pi^0 \tau^+ \nu_\tau)$ is one order smaller than previous one in Ref. [76].
- In addition, the lepton flavor universality parameters $R^{\mu/e}(D \rightarrow P \ell^+ \nu_\ell)$ are also given in Tab. II, since many terms are canceled in the ratios, these predictions are quite accurate, and all processes have similar results.

For the q^2 dependence of the differential branching ratios of the $D \rightarrow P \ell^+ \nu_\ell$ decays with present experimental bounds, we only show the not yet measured processes $D^+ \rightarrow \eta' \mu^+ \nu_\mu$, $D_s^+ \rightarrow K^0 \mu^+ \nu_\mu$, $D_s^+ \rightarrow \pi^0 \mu^+ \nu_\mu$ and $D_s^+ \rightarrow \pi^0 \tau^+ \nu_\tau$ in Fig. 1. We do not show $d\mathcal{B}(D_s^+ \rightarrow \pi^0 e^+ \nu_e)/dq^2$, since it is similar to $d\mathcal{B}(D_s^+ \rightarrow \pi^0 \mu^+ \nu_\mu)/dq^2$ in Fig. 1

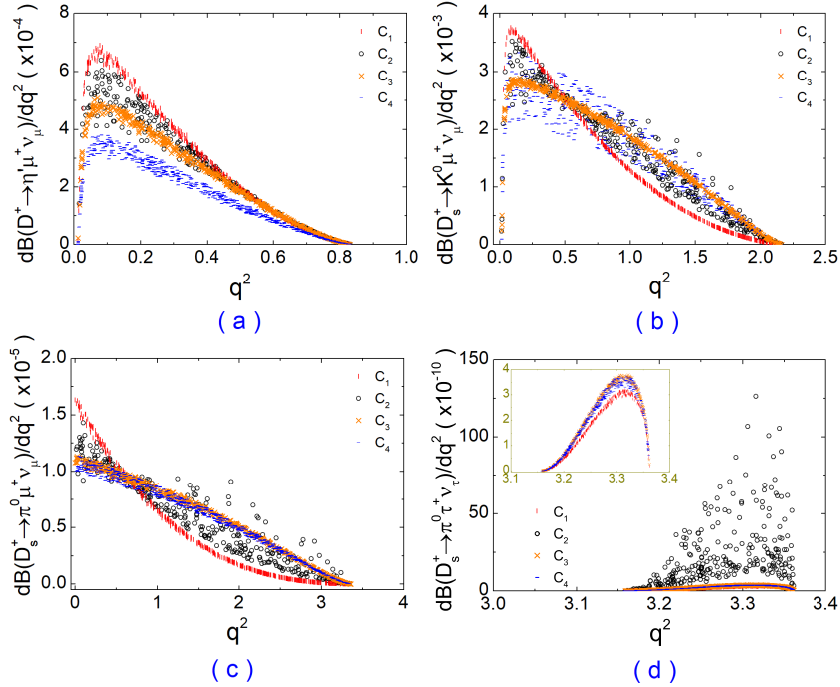


FIG. 1: The q^2 dependence of the differential branching ratios for some $D \rightarrow P \ell^+ \nu_\ell$ with present experimental bounds.

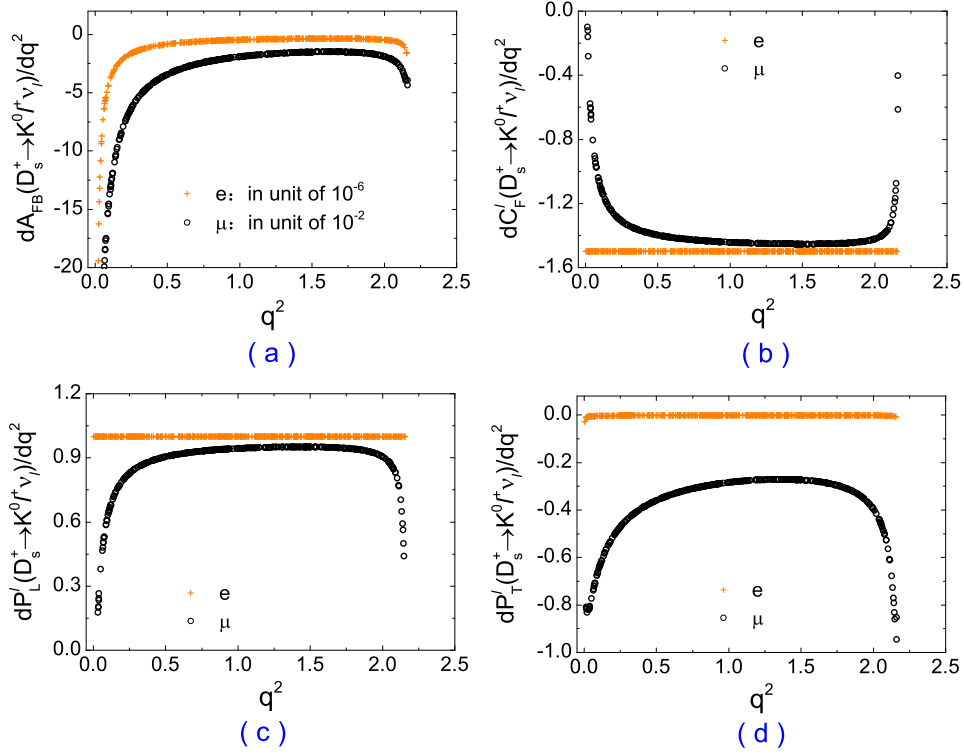


FIG. 2: The differential forward-backward asymmetries, differential lepton-side convexity parameters, differential longitudinal lepton polarizations and differential transverse lepton polarizations for the $D_s^+ \rightarrow K^0 \ell^+ \nu_\ell$ decays in the C_3 case.

(c). From Fig. 1, one can see that present experimental measurements give quite strong bounds on the differential branching ratios of $D^+ \rightarrow \eta' \mu^+ \nu_\mu$, $D_s^+ \rightarrow \pi^0 \mu^+ \nu_\mu$ and $D_s^+ \rightarrow \pi^0 \tau^+ \nu_\tau$ decays in the C_1 , C_3 and C_4 cases as well as $D_s^+ \rightarrow K^0 \mu^+ \nu_\mu$ decays in the C_1 and C_3 cases, and all predictions of the four differential branching ratios in the C_2 case have large error due to the form factor choice. Comparing with $d\mathcal{B}(D_s^+ \rightarrow \pi^0 \mu^+ \nu_\mu)/dq^2$ in Fig. 1 (c), as shown in Fig. 1 (d), $d\mathcal{B}(D_s^+ \rightarrow \pi^0 \tau^+ \nu_\tau)/dq^2$ is suppressed about the order of $\mathcal{O}(10^{-4})$ by m_τ .

The forward-backward asymmetries A_{FB}^ℓ , the lepton-side convexity parameters C_F^ℓ , the longitudinal polarizations of the final charged leptons P_L^ℓ and the transverse polarizations of the final charged leptons P_T^ℓ with two ways of integration for the $D \rightarrow P \ell^+ \nu_\ell$ decays could also be obtained. These predictions are very accurate, and they are similar to each other in the four $C_{1,2,3,4}$ cases. So we only give the predictions within the C_3 case in Tab. III for examples. From Tab. III, one can see that the predictions are obviously different between two ways of q^2 integration, and the slight difference in the same way of q^2 integration is due to the different decay phase spaces. For displaying the differences between the $D \rightarrow P e^+ \nu_e$ and $D \rightarrow P \mu^+ \nu_\mu$ decays, we take $D_s^+ \rightarrow K^0 e^+ \nu_e$ and $D_s^+ \rightarrow K^0 \mu^+ \nu_\mu$ as examples. The differential forward-backward asymmetries, the differential lepton-side convexity parameters, the differential longitudinal lepton polarizations and the differential transverse lepton polarizations of $D_s^+ \rightarrow K^0 e^+ \nu_e$ and $D_s^+ \rightarrow K^0 \mu^+ \nu_\mu$ decays within the C_3 case are displayed in Fig. 2. And one can see that differential observables between $\ell = e$ and $\ell = \mu$ are obviously different, specially in the low and high q^2 ranges.

TABLE III: Quantities $\langle X \rangle$ and \overline{X} of the $D \rightarrow P\ell^+\nu$ in C_3 case.

Decay modes	$\langle A_{FB}^\ell \rangle$	$\frac{\overline{A_{FB}^\ell}(\times 10^{-6})}{A_{FB}^{\mu,\tau}(\times 10^{-2})}$	$\langle C_F^\ell \rangle$	$\overline{C_F^\ell}$	$\langle P_L^\ell \rangle$	$\overline{P_L^\ell}$	$\langle P_T^\ell \rangle$	$\frac{\overline{P_T^\ell}(\times 10^{-3})}{P_T^{\mu,\tau}}$
$D^+ \rightarrow \overline{K}^0 e^+ \nu_e$	-0.087	-3.254 ± 0.001	-1.239	-1.500	0.768	1.000	-0.273	-2.442 ± 0.001
$D^+ \rightarrow \pi^0 e^+ \nu_e$	-0.083	-2.054 ± 0.000	-1.252	-1.500	0.780	1.000	-0.260	-1.730 ± 0.000
$D^+ \rightarrow \eta e^+ \nu_e$	-0.087	-3.476 ± 0.001	-1.239	-1.500	0.768	1.000	-0.273	-2.490 ± 0.000
$D^+ \rightarrow \eta' e^+ \nu_e$	-0.093	-7.075 ± 0.003	-1.222	-1.500	0.753	1.000	-0.290	-3.890 ± 0.001
$D^0 \rightarrow K^- e^+ \nu_e$	-0.087	-3.259 ± 0.001	-1.239	-1.500	0.768	1.000	-0.273	-2.446 ± 0.001
$D^0 \rightarrow \pi^- e^+ \nu_e$	-0.083	-2.077 ± 0.000	-1.252	-1.500	0.779	1.000	-0.260	-1.751 ± 0.000
$D_s^+ \rightarrow \eta e^+ \nu_e$	-0.086	-3.033 ± 0.001	-1.242	-1.500	0.770	1.000	-0.270	-2.300 ± 0.001
$D_s^+ \rightarrow \eta' e^+ \nu_e$	-0.091	-5.829 ± 0.003	-1.226	-1.500	0.757	1.000	-0.286	-3.484 ± 0.001
$D_s^+ \rightarrow K^0 e^+ \nu_e$	-0.085	-2.814 ± 0.001	-1.245	-1.500	0.773	1.000	-0.267	-2.118 ± 0.000
$D_s^+ \rightarrow \pi^0 e^+ \nu_e$	-0.082	-1.850 ± 0.001	-1.254	-1.500	0.781	1.000	-0.258	-1.634 ± 0.001
$D^+ \rightarrow \overline{K}^0 \mu^+ \nu_\mu$	-0.226	-4.278 ± 0.001	-0.822	-1.352	0.394	0.851	-0.655	-0.414
$D^+ \rightarrow \pi^0 \mu^+ \nu_\mu$	-0.201	-2.810 ± 0.000	-0.897	-1.405	0.462	0.907	-0.602	-0.310
$D^+ \rightarrow \eta \mu^+ \nu_\mu$	-0.227	-4.490 ± 0.001	-0.819	-1.347	0.391	0.846	-0.657	-0.419
$D^+ \rightarrow \eta' \mu^+ \nu_\mu$	-0.263	-8.097 ± 0.003	-0.708	-1.213	0.287	0.703	-0.725	-0.581
$D^0 \rightarrow K^- \mu^+ \nu_\mu$	-0.226	-4.285 ± 0.001	-0.822	-1.352	0.393	0.850	-0.656	-0.414
$D^0 \rightarrow \pi^- \mu^+ \nu_\mu$	-0.201	-2.844 ± 0.001	-0.895	-1.407	0.461	0.910	-0.603	-0.313
$D_s^+ \rightarrow \eta \mu^+ \nu_\mu$	-0.221	-4.001 ± 0.001	-0.836	-1.364	0.406	0.864	-0.646	-0.394
$D_s^+ \rightarrow \eta' \mu^+ \nu_\mu$	-0.254	-6.952 ± 0.003	-0.736	-1.254	0.314	0.747	-0.709	-0.540
$D_s^+ \rightarrow K^0 \mu^+ \nu_\mu$	-0.215	-3.701 ± 0.001	-0.856	-1.377	0.425	0.879	-0.632	-0.367
$D_s^+ \rightarrow \pi^0 \mu^+ \nu_\mu$	-0.197	-2.571 ± 0.001	-0.907	-1.417	0.472	0.920	-0.594	-0.295
$D_s^+ \rightarrow \pi^0 \tau^+ \nu_\tau$	-0.281	-27.429 ± 0.105	-0.211 ± 0.003	-0.212 ± 0.003	-0.868 ± 0.001	-0.873 ± 0.001	-0.447 ± 0.002	-0.437 ± 0.002

B. $D \rightarrow V\ell^+\nu_\ell$ decays

The hadronic helicity amplitudes for the $D \rightarrow V\ell^+\nu_\ell$ decays are given in Tab. IV. There are four nonperturbative parameters $B_{1,2,3,4}$ in the $D \rightarrow V\ell^+\nu_\ell$ decay modes. If neglecting the SU(3) flavor breaking c_1^V and c_2^V terms, $B_1 = B_2 = B_3 = B_4 = c_0^V$, and then all hadronic helicity amplitudes of $D \rightarrow V\ell^+\nu_\ell$ are related by only one parameter c_0^V .

Among the $D \rightarrow V\ell^+\nu_\ell$ decay modes, 13 branching ratios have been measured, and 2 branching ratios have been upper limited by the experiments. The experimental data with 2σ errors are listed in the second column of Tab. V. Now we use the listed experimental data to constrain the parameters B_i and then predict other not yet measured and not yet well measured branching ratios. The numerical results of $\mathcal{B}(D \rightarrow V\ell^+\nu_\ell)$ in the C_1 , C_2 , C_3 and C_4 cases are given in the third, forth, fifth and sixth columns of Tab. V, respectively.

The results in the C_1 , C_2 and C_3 cases are very similar. Since the SU(3) flavor symmetry predictions of $\mathcal{B}(D^+ \rightarrow \omega e^+ \nu_e)$ and $\mathcal{B}(D^0 \rightarrow \rho^- \mu^+ \nu_\mu)$ are slightly larger than their experimental data within 2σ errors in the three cases, we

TABLE IV: The hadronic helicity amplitudes for $D \rightarrow V\ell^+\nu$ decays including both the SU(3) flavor symmetry and the SU(3) flavor breaking contributions. $B_1 = c_0^V + c_1^V - 2c_2^V$, $B_2 = c_0^V - 2c_1^V - 2c_2^V$, $B_3 = c_0^V + c_1^V + c_2^V$, $B_4 = c_0^V - 2c_1^V + c_2^V$. If neglecting the SU(3) flavor breaking c_1^V and c_2^V terms, $B_1 = B_2 = B_3 = B_4 = c_0^V$.

Hadronic helicity amplitudes	SU(3) IRA amplitudes
$H(D^0 \rightarrow K^{*-}\ell^+\nu_\ell)$	$B_1 V_{cs}^*$
$H(D^+ \rightarrow \bar{K}^{*0}\ell^+\nu_\ell)$	$B_1 V_{cs}^*$
$H(D_s^+ \rightarrow \phi\ell^+\nu_\ell)$	$(-\cos\theta_V \sqrt{2/3} - \sin\theta_V/\sqrt{3}) B_2 V_{cs}^*$
$H(D_s^+ \rightarrow \omega\ell^+\nu_\ell)$	$(-\sin\theta_V \sqrt{2/3} + \cos\theta_V/\sqrt{3}) B_2 V_{cs}^*$
$H(D^0 \rightarrow \rho^-\ell^+\nu_\ell)$	$B_3 V_{cd}^*$
$H(D^+ \rightarrow \rho^0\ell^+\nu_\ell)$	$-\frac{1}{\sqrt{2}} B_3 V_{cd}^*$
$H(D^+ \rightarrow \phi\ell^+\nu_\ell)$	$(\cos\theta_V/\sqrt{6} - \sin\theta_V/\sqrt{3}) B_3 V_{cd}^*$
$H(D^+ \rightarrow \omega\ell^+\nu_\ell)$	$(\sin\theta_V/\sqrt{6} + \cos\theta_V/\sqrt{3}) B_3 V_{cd}^*$
$H(D_s^+ \rightarrow K^{*0}\ell^+\nu_\ell)$	$B_4 V_{cd}^*$

do not use them to constrain the nonperturbative parameter c_0^V . One can see that the prediction of $\mathcal{B}(D^0 \rightarrow \rho^-\mu^+\nu_\mu)$ is agree with its experimental data within 3σ errors, nevertheless, the prediction of $\mathcal{B}(D^+ \rightarrow \omega e^+\nu_e)$ still slightly larger than experimental data within 3σ errors. $\mathcal{B}(D_s^+ \rightarrow K^{*0}\mu^+\nu_\mu)$ and $\mathcal{B}(D_s^+ \rightarrow \omega e^+\nu_e, \omega\mu^+\nu_\mu)$ are predicted on the order of $\mathcal{O}(10^{-3})$ and $\mathcal{O}(10^{-5})$, respectively. And they could be measured in BESIII, LHCb and BelleII experiments. In the C_4 case, as given in the sixth column of Tab. V, after considering both the hadronic momentum-transfer q^2 dependence of the form factors and the SU(3) flavor breaking contributions, all SU(3) flavor symmetry predictions are consistent with their experimental data within 2σ errors. Among relevant not yet measured decays, $\mathcal{B}(D_s^+ \rightarrow K^{*0}\mu^+\nu_\mu)$ is calculated in the SM using light-cone sum rules [79] and in the relativistic quark model [7], $\mathcal{B}(D_s^+ \rightarrow K^{*0}\mu^+\nu_\mu) = (2.23 \pm 0.32) \times 10^{-3}$ [79] and 2.0×10^{-3} [7], and our predictions of $\mathcal{B}(D_s^+ \rightarrow K^{*0}\mu^+\nu_\mu)$ in the C_1, C_2, C_3 and C_4 cases are coincident with previous ones in Refs. [7, 79]. In addition, the lepton flavor universality parameters $R^{\mu/e}(D \rightarrow V\ell^+\nu_\ell)$ are also given in Tab. V. Since many terms are canceled in the ratios, these predictions of the lepton flavor universality parameters are quite accurate, and our predictions in all four cases are similar to each other.

For the q^2 dependence of the differential branching ratios of the $D \rightarrow V\ell^+\nu_\ell$ decays with present experimental bounds, we only show the not yet measured processes $D^+ \rightarrow \phi\mu^+\nu_\mu$, $D_s^+ \rightarrow \omega\mu^+\nu_\mu$ and $D_s^+ \rightarrow K^{*0}\mu^+\nu_\mu$ in Fig. 3. The differential branching ratios of $D^+ \rightarrow \phi e^+\nu_e$ ($D_s^+ \rightarrow \omega e^+\nu_e$) is similar to $D^+ \rightarrow \phi\mu^+\nu_\mu$ ($D_s^+ \rightarrow \omega\mu^+\nu_\mu$), so we do not shown them in Fig. 3. From Fig. 3, one can see that present experiment data give quite strong bounds on all differential branching ratios of $D^+ \rightarrow \phi\mu^+\nu_\mu$, $D_s^+ \rightarrow \omega\mu^+\nu_\mu$ and $D_s^+ \rightarrow K^{*0}\mu^+\nu_\mu$ decays in the C_1, C_2 and C_3 cases. The prediction of $d\mathcal{B}(D^+ \rightarrow \phi\mu^+\nu_\mu)/dq^2$ in the C_4 case could be distinguished from ones in the $C_{1,2,3}$ cases within the middle range of q^2 . And the error of $d\mathcal{B}(D_s^+ \rightarrow K^{*0}\mu^+\nu_\mu)/dq^2$ in the C_4 case is obviously larger than ones in $C_{1,2,3}$ cases.

The forward-backward asymmetries A_{FB}^ℓ , the lepton-side convexity parameters C_F^ℓ , the longitudinal polarizations P_L^ℓ , the transverse polarizations P_T^ℓ , the lepton spin asymmetries A_λ and the longitudinal polarization fractions of the final vector mesons F_L with two ways of integration have also been predicted in the four cases. Since many theoretical

TABLE V: Branching ratios of the $D \rightarrow V\ell^+\nu$ within 2σ errors. † The experimental data of $\mathcal{B}(D^+ \rightarrow \omega e^+\nu_e)$ and $\mathcal{B}(D^0 \rightarrow \rho^-\mu^+\nu_\mu)$ from PDG [1] are not used in the $C_{1,2,3}$ cases.

Branching ratios	Exp. data	Ones in C_1	Ones in C_2	Ones in C_3	Ones in C_4
$\mathcal{B}(D^+ \rightarrow \bar{K}^{*0} e^+\nu_e)(\times 10^{-2})$	5.40 ± 0.20	5.44 ± 0.15	5.42 ± 0.18	5.36 ± 0.08	5.44 ± 0.16
$\mathcal{B}(D^+ \rightarrow \rho^0 e^+\nu_e)(\times 10^{-3})$	$2.18^{+0.34}_{-0.50}$	2.31 ± 0.07	2.39 ± 0.13	2.33 ± 0.05	1.83 ± 0.15
$\mathcal{B}(D^+ \rightarrow \omega e^+\nu_e)(\times 10^{-3})$	1.69 ± 0.22	$2.24 \pm 0.07^\dagger$	$2.33 \pm 0.12^\dagger$	$2.26 \pm 0.04^\dagger$	1.77 ± 0.14
$\mathcal{B}(D^+ \rightarrow \phi e^+\nu_e)(\times 10^{-7})$	< 130	3.13 ± 0.12	3.11 ± 0.19	3.07 ± 0.07	2.38 ± 0.23
$\mathcal{B}(D^0 \rightarrow K^{*-} e^+\nu_e)(\times 10^{-2})$	2.15 ± 0.32	2.12 ± 0.09	2.13 ± 0.10	2.08 ± 0.06	2.13 ± 0.10
$\mathcal{B}(D^0 \rightarrow \rho^- e^+\nu_e)(\times 10^{-3})$	1.50 ± 0.24	1.79 ± 0.08	1.86 ± 0.11	1.80 ± 0.06	1.41 ± 0.13
$\mathcal{B}(D_s^+ \rightarrow \phi e^+\nu_e)(\times 10^{-2})$	2.39 ± 0.32	2.46 ± 0.12	2.43 ± 0.14	2.40 ± 0.10	2.39 ± 0.32
$\mathcal{B}(D_s^+ \rightarrow \omega e^+\nu_e)(\times 10^{-5})$	< 200	2.45 ± 0.13	2.56 ± 0.20	2.47 ± 0.10	2.49 ± 0.38
$\mathcal{B}(D_s^+ \rightarrow K^{*0} e^+\nu_e)(\times 10^{-3})$	2.15 ± 0.56	2.17 ± 0.10	2.25 ± 0.13	2.17 ± 0.08	2.15 ± 0.56
$\mathcal{B}(D^+ \rightarrow \bar{K}^{*0} \mu^+\nu_\mu)(\times 10^{-2})$	5.27 ± 0.30	5.12 ± 0.15	5.13 ± 0.16	5.05 ± 0.08	5.12 ± 0.15
$\mathcal{B}(D^+ \rightarrow \rho^0 \mu^+\nu_\mu)(\times 10^{-3})$	2.4 ± 0.8	2.19 ± 0.07	2.29 ± 0.13	2.22 ± 0.04	1.74 ± 0.14
$\mathcal{B}(D^+ \rightarrow \omega \mu^+\nu_\mu)(\times 10^{-3})$	1.77 ± 0.42	2.13 ± 0.06	2.23 ± 0.12	2.15 ± 0.04	1.68 ± 0.13
$\mathcal{B}(D^+ \rightarrow \phi \mu^+\nu_\mu)(\times 10^{-7})$	\dots	2.89 ± 0.11	2.89 ± 0.17	2.84 ± 0.07	2.20 ± 0.21
$\mathcal{B}(D^0 \rightarrow K^{*-} \mu^+\nu_\mu)(\times 10^{-2})$	1.89 ± 0.48	1.99 ± 0.09	2.01 ± 0.09	1.96 ± 0.06	2.01 ± 0.10
$\mathcal{B}(D^0 \rightarrow \rho^- \mu^+\nu_\mu)(\times 10^{-3})$	1.35 ± 0.26	$1.70 \pm 0.07^\dagger$	$1.78 \pm 0.11^\dagger$	$1.72 \pm 0.06^\dagger$	1.34 ± 0.13
$\mathcal{B}(D_s^+ \rightarrow \phi \mu^+\nu_\mu)(\times 10^{-2})$	1.9 ± 1.0	2.30 ± 0.12	2.29 ± 0.12	2.25 ± 0.09	2.24 ± 0.30
$\mathcal{B}(D_s^+ \rightarrow \omega \mu^+\nu_\mu)(\times 10^{-5})$	\dots	2.34 ± 0.12	2.47 ± 0.19	2.37 ± 0.09	2.38 ± 0.36
$\mathcal{B}(D_s^+ \rightarrow K^{*0} \mu^+\nu_\mu)(\times 10^{-3})$	\dots	2.06 ± 0.10	2.15 ± 0.13	2.07 ± 0.08	2.05 ± 0.53
$R^{\mu/e}(D^+ \rightarrow \bar{K}^{*0} \ell^+\nu_\ell)$		0.939 ± 0.001	0.944 ± 0.004	0.941 ± 0.001	0.941 ± 0.001
$R^{\mu/e}(D^+ \rightarrow \rho^0 \ell^+\nu_\ell)$		0.950 ± 0.001	0.956 ± 0.005	0.952 ± 0.001	0.952 ± 0.001
$R^{\mu/e}(D^+ \rightarrow \omega \ell^+\nu_\ell)$		0.950 ± 0.001	0.956 ± 0.005	0.952 ± 0.001	0.952 ± 0.001
$R^{\mu/e}(D^+ \rightarrow \phi \ell^+\nu_\ell)$		0.923 ± 0.001	0.928 ± 0.005	0.925 ± 0.001	0.925 ± 0.001
$R^{\mu/e}(D^0 \rightarrow K^{*-} \ell^+\nu_\ell)$		0.939 ± 0.001	0.944 ± 0.004	0.941 ± 0.001	0.941 ± 0.001
$R^{\mu/e}(D^0 \rightarrow \rho^- \ell^+\nu_\ell)$		0.950 ± 0.001	0.956 ± 0.005	0.952 ± 0.001	0.952 ± 0.001
$R^{\mu/e}(D_s^+ \rightarrow \phi \ell^+\nu_\ell)$		0.937 ± 0.001	0.942 ± 0.004	0.939 ± 0.001	0.939 ± 0.001
$R^{\mu/e}(D_s^+ \rightarrow \omega \ell^+\nu_\ell)$		0.957 ± 0.001	0.963 ± 0.004	0.959 ± 0.001	0.959 ± 0.001
$R^{\mu/e}(D_s^+ \rightarrow K^{*0} \ell^+\nu_\ell)$		0.949 ± 0.001	0.955 ± 0.005	0.951 ± 0.001	0.951 ± 0.001

uncertainties are canceled in the ratios, these predictions are very accurate. These predictions are similar to each other in the four cases, and we only list the results in the C_3 case in Tabs. VI-VII for examples. One can see that the predictions are obviously different between two ways of q^2 integration, and they are also quite different between $D \rightarrow Ve^+\nu_e$ and $D \rightarrow V\mu^+\nu_\mu$ decays.

The differential observables of $D_s^+ \rightarrow K^{*0}\ell^+\nu_\ell$ decays in the C_3 case are displayed in Fig. 4. One can see that, in the low q^2 ranges, the differential observables $\text{expect } dF_L(D_s^+ \rightarrow K^{*0}\ell^+\nu_\ell)/dq^2$ are obviously different between decays with $\ell = e$ and $\ell = \mu$.

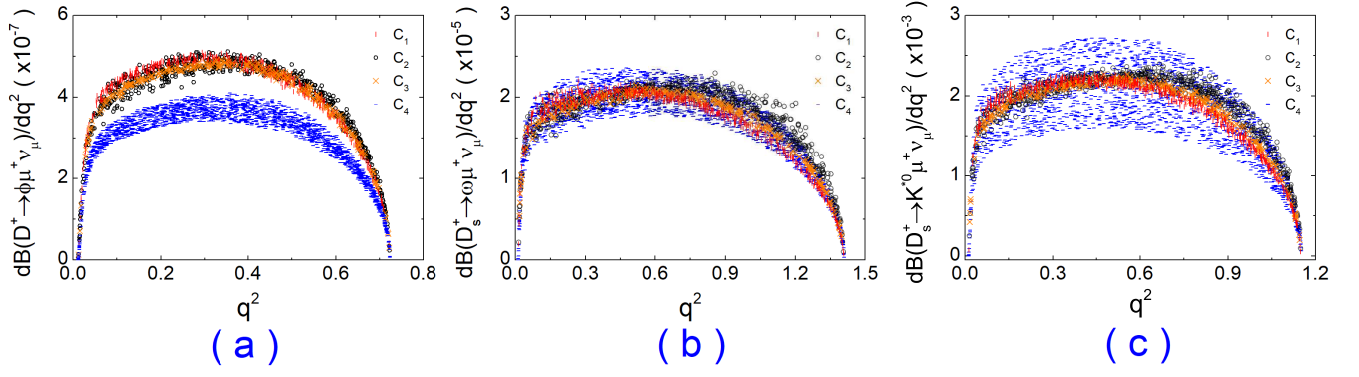


FIG. 3: The q^2 dependence of the differential branching ratios for some not yet measured $D \rightarrow V\mu^+\nu_\mu$ decays with present experimental bounds.

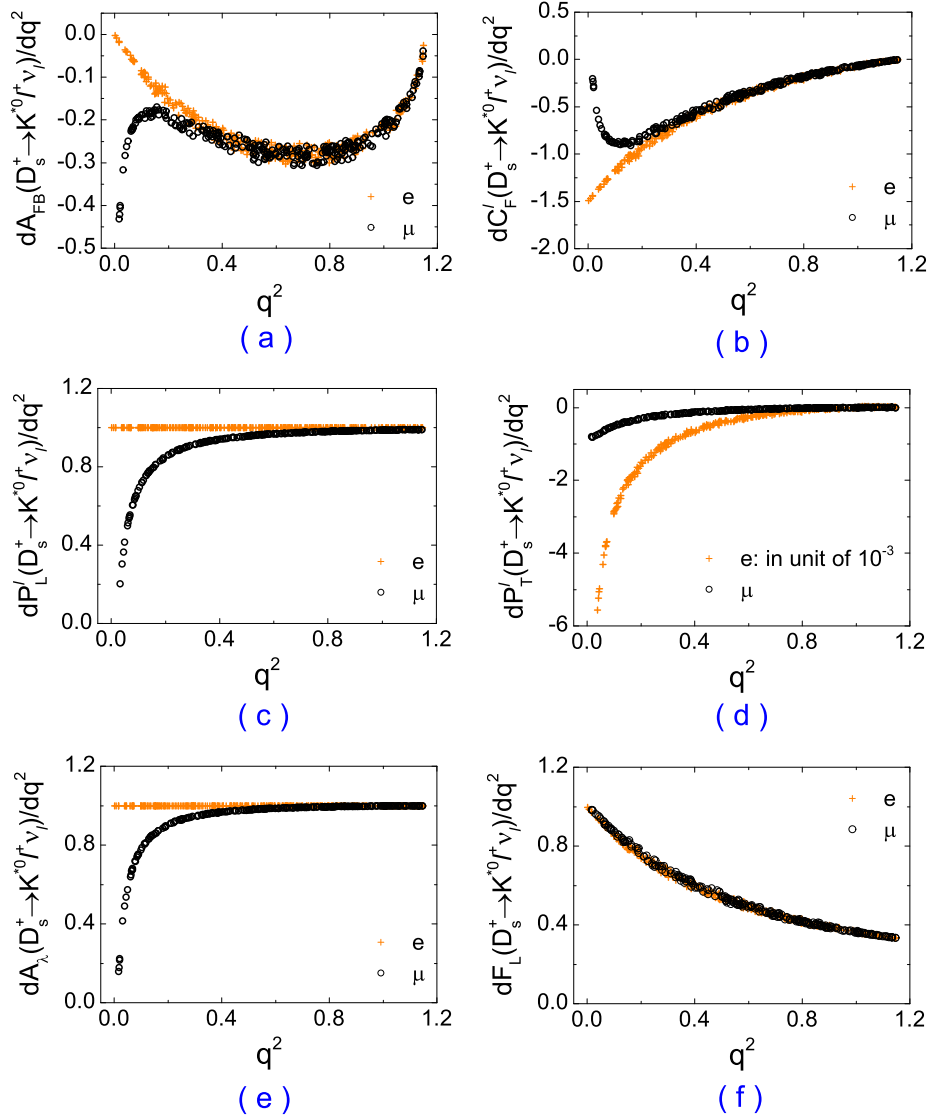


FIG. 4: The differential forward-backward asymmetries, differential lepton-side convexity parameters, differential longitudinal lepton polarizations and differential transverse lepton polarizations for the $D_s^+ \rightarrow K^0 \ell^+ \nu_\ell$ decays in the C_3 case.

TABLE VI: The forward-backward asymmetries A_{FB}^ℓ , the lepton-side convexity parameters C_F^ℓ , the longitudinal polarizations P_L^ℓ of the $D \rightarrow V\ell^+\nu$ decays in the C_3 case.

Decay modes	$\langle A_{FB}^\ell \rangle$	$\overline{A_{FB}^\ell}$	$\langle C_F^\ell \rangle$	$\overline{C_F^\ell}$	$\langle P_L^\ell \rangle$	$\overline{P_L^\ell}$
$D^+ \rightarrow \overline{K}^{*0} e^+ \nu_e$	-0.125 ± 0.006	-0.190 ± 0.020	-1.046 ± 0.019	-0.500 ± 0.032	0.786 ± 0.004	1.000
$D^+ \rightarrow \rho^0 e^+ \nu_e$	-0.130 ± 0.008	-0.222 ± 0.024	-1.052 ± 0.023	-0.496 ± 0.041	0.789 ± 0.004	1.000
$D^+ \rightarrow \omega e^+ \nu_e$	-0.130 ± 0.008	-0.220 ± 0.024	-1.052 ± 0.023	-0.497 ± 0.041	0.789 ± 0.004	1.000
$D^+ \rightarrow \phi e^+ \nu_e$	-0.121 ± 0.005	-0.164 ± 0.017	-1.037 ± 0.015	-0.500 ± 0.025	0.784 ± 0.003	1.000
$D^0 \rightarrow K^{*-} e^+ \nu_e$	-0.125 ± 0.006	-0.191 ± 0.020	-1.046 ± 0.019	-0.500 ± 0.032	0.786 ± 0.004	1.000
$D^0 \rightarrow \rho^- e^+ \nu_e$	-0.130 ± 0.008	-0.221 ± 0.024	-1.052 ± 0.023	-0.497 ± 0.041	0.789 ± 0.004	1.000
$D_s^+ \rightarrow \phi e^+ \nu_e$	-0.122 ± 0.006	-0.176 ± 0.018	-1.043 ± 0.016	-0.500 ± 0.028	0.786 ± 0.003	1.000
$D_s^+ \rightarrow \omega e^+ \nu_e$	-0.130 ± 0.008	-0.229 ± 0.025	-1.057 ± 0.025	-0.496 ± 0.044	0.790 ± 0.004	1.000
$D_s^+ \rightarrow K^{*0} e^+ \nu_e$	-0.128 ± 0.007	-0.207 ± 0.022	-1.049 ± 0.021	-0.495 ± 0.036	0.789 ± 0.004	1.000
$D^+ \rightarrow \overline{K}^{*0} \mu^+ \nu_\mu$	-0.284 ± 0.009	-0.226 ± 0.019	-0.466 ± 0.021	-0.395 ± 0.028	0.514 ± 0.017	0.886 ± 0.002
$D^+ \rightarrow \rho^0 \mu^+ \nu_\mu$	-0.292 ± 0.011	-0.252 ± 0.023	-0.491 ± 0.027	-0.405 ± 0.037	0.524 ± 0.020	0.903 ± 0.002
$D^+ \rightarrow \omega \mu^+ \nu_\mu$	-0.292 ± 0.011	-0.251 ± 0.022	-0.490 ± 0.027	-0.405 ± 0.037	0.524 ± 0.020	0.902 ± 0.002
$D^+ \rightarrow \phi \mu^+ \nu_\mu$	-0.277 ± 0.008	-0.206 ± 0.016	-0.433 ± 0.016	-0.376 ± 0.021	0.503 ± 0.014	0.864 ± 0.002
$D^0 \rightarrow K^{*-} \mu^+ \nu_\mu$	-0.284 ± 0.009	-0.226 ± 0.019	-0.466 ± 0.021	-0.395 ± 0.029	0.514 ± 0.017	0.886 ± 0.002
$D^0 \rightarrow \rho^- \mu^+ \nu_\mu$	-0.292 ± 0.011	-0.252 ± 0.023	-0.490 ± 0.027	-0.405 ± 0.037	0.524 ± 0.020	0.902 ± 0.002
$D_s^+ \rightarrow \phi \mu^+ \nu_\mu$	-0.277 ± 0.008	-0.213 ± 0.017	-0.459 ± 0.018	-0.391 ± 0.024	0.514 ± 0.015	0.882 ± 0.002
$D_s^+ \rightarrow \omega \mu^+ \nu_\mu$	-0.291 ± 0.012	-0.257 ± 0.024	-0.509 ± 0.029	-0.414 ± 0.041	0.531 ± 0.021	0.913 ± 0.002
$D_s^+ \rightarrow K^{*0} \mu^+ \nu_\mu$	-0.286 ± 0.010	-0.239 ± 0.021	-0.485 ± 0.024	-0.402 ± 0.033	0.525 ± 0.018	0.900 ± 0.002

TABLE VII: The transverse polarizations P_T^ℓ , the lepton spin asymmetries A_λ and the longitudinal polarization fractions of the final vector mesons F_L of the $D \rightarrow V\ell^+\nu$ decays in the C_3 case.

Decay modes	$\langle P_T^\ell \rangle$	$\frac{\overline{P_T^\ell} (\times 10^{-3})}{P_T^\mu}$	$\langle A_\lambda \rangle$	$\overline{A_\lambda}$	$\langle F_L \rangle$	$\overline{F_L}$
$D^+ \rightarrow \overline{K}^{*0} e^+ \nu_e$	-0.251 ± 0.004	-1.205 ± 0.066	1.000	1.000	0.905 ± 0.010	0.556 ± 0.014
$D^+ \rightarrow \rho^0 e^+ \nu_e$	-0.249 ± 0.005	-1.040 ± 0.072	1.000	1.000	0.907 ± 0.012	0.554 ± 0.018
$D^+ \rightarrow \omega e^+ \nu_e$	-0.249 ± 0.005	-1.049 ± 0.073	1.000	1.000	0.907 ± 0.012	0.554 ± 0.018
$D^+ \rightarrow \phi e^+ \nu_e$	-0.254 ± 0.003	-1.417 ± 0.061	1.000	1.000	0.902 ± 0.008	0.556 ± 0.011
$D^0 \rightarrow K^{*-} e^+ \nu_e$	-0.251 ± 0.004	-1.206 ± 0.067	1.000	1.000	0.905 ± 0.010	0.556 ± 0.014
$D^0 \rightarrow \rho^- e^+ \nu_e$	-0.249 ± 0.005	-1.045 ± 0.073	1.000	1.000	0.907 ± 0.012	0.554 ± 0.018
$D_s^+ \rightarrow \phi e^+ \nu_e$	-0.251 ± 0.004	-1.255 ± 0.060	1.000	1.000	0.904 ± 0.009	0.555 ± 0.012
$D_s^+ \rightarrow \omega e^+ \nu_e$	-0.247 ± 0.005	-0.953 ± 0.071	1.000	1.000	0.908 ± 0.013	0.554 ± 0.020
$D_s^+ \rightarrow K^{*0} e^+ \nu_e$	-0.248 ± 0.004	-1.075 ± 0.066	1.000	1.000	0.905 ± 0.011	0.553 ± 0.016
$D^+ \rightarrow \overline{K}^{*0} \mu^+ \nu_\mu$	-0.454 ± 0.022	-0.156 ± 0.012	0.935 ± 0.005	0.928 ± 0.002	0.775 ± 0.019	0.557 ± 0.014
$D^+ \rightarrow \rho^0 \mu^+ \nu_\mu$	-0.452 ± 0.026	-0.139 ± 0.014	0.944 ± 0.006	0.937 ± 0.002	0.782 ± 0.023	0.555 ± 0.018
$D^+ \rightarrow \omega \mu^+ \nu_\mu$	-0.452 ± 0.026	-0.140 ± 0.014	0.944 ± 0.006	0.937 ± 0.002	0.782 ± 0.023	0.555 ± 0.018
$D^+ \rightarrow \phi \mu^+ \nu_\mu$	-0.455 ± 0.018	-0.175 ± 0.011	0.924 ± 0.005	0.915 ± 0.002	0.763 ± 0.015	0.557 ± 0.011
$D^0 \rightarrow K^{*-} \mu^+ \nu_\mu$	-0.454 ± 0.022	-0.156 ± 0.012	0.935 ± 0.005	0.927 ± 0.002	0.775 ± 0.019	0.557 ± 0.014
$D^0 \rightarrow \rho^- \mu^+ \nu_\mu$	-0.452 ± 0.026	-0.140 ± 0.014	0.944 ± 0.006	0.937 ± 0.002	0.782 ± 0.023	0.555 ± 0.018
$D_s^+ \rightarrow \phi \mu^+ \nu_\mu$	-0.454 ± 0.019	-0.162 ± 0.011	0.934 ± 0.005	0.925 ± 0.002	0.771 ± 0.016	0.557 ± 0.012
$D_s^+ \rightarrow \omega \mu^+ \nu_\mu$	-0.452 ± 0.027	-0.131 ± 0.014	0.950 ± 0.005	0.943 ± 0.002	0.788 ± 0.024	0.555 ± 0.019
$D_s^+ \rightarrow K^{*0} \mu^+ \nu_\mu$	-0.451 ± 0.023	-0.143 ± 0.012	0.943 ± 0.005	0.936 ± 0.002	0.779 ± 0.021	0.555 ± 0.016

C. $D \rightarrow S\ell^+\nu_\ell$ decays

For $D \rightarrow S\ell^+\nu_\ell$ decays, the two quark and the four quark scenarios for the scalar mesons below or near 1 GeV are considered. The hadronic helicity amplitudes for the $D \rightarrow S\ell^+\nu_\ell$ decays are given in Tab. VIII, in which the CKM matrix element V_{cs} and V_{cd} information are kept for comparing conveniently. There are four (five) nonperturbative parameters $E_{1,2,3,4}$ ($E'_{1,2,3,4,5}$) in the two quark (four quark) picture. After ignoring the SU(3) flavor breaking contributions, only one nonperturbative parameter $E_1 = E_2 = E_3 = E_4 = c_0^S$ or $E'_1 = E'_2 = E'_3 = E'_4 = E'_5 = c_0'^S$ relates all decay amplitudes in the two quark or the four quark picture, respectively.

Unlike many measured decay modes in the $D \rightarrow P\ell^+\nu_\ell$ and $D \rightarrow V\ell^+\nu_\ell$ decays, among these $D \rightarrow S\ell^+\nu_\ell$ decays, only $D_s^+ \rightarrow f_0(980)e^+\nu_e$ decay has been measured, and its branching ratio with 2σ errors is [1]

$$\mathcal{B}(D_s^+ \rightarrow f_0(980)e^+\nu_e) = (2.3 \pm 0.8) \times 10^{-3}. \quad (48)$$

In addition, the branching ratios of the $D \rightarrow P_1P_2\ell^+\nu_\ell$ decays with the light scalar resonances can be obtained by using $\mathcal{B}(D \rightarrow S\ell^+\nu_\ell)$ and $\mathcal{B}(S \rightarrow P_1P_2)$, and the detail analysis can be found in Ref. [80]. Five branching ratios

TABLE VIII: The hadronic helicity amplitudes for $D \rightarrow S\ell^+\nu$ decays including both the SU(3) flavor symmetry and the SU(3) flavor breaking contributions. In the two quark picture of the scalar mesons, $E_1 \equiv c_0^S + c_1^S - 2c_2^S$, $E_2 \equiv c_0^S - 2c_1^S - 2c_2^S$, $E_3 \equiv c_0^S + c_1^S + c_2^S$, $E_4 \equiv c_0^S - 2c_1^S + c_2^S$. $E_1 = E_2 = E_3 = E_4 = c_0^S$ if neglecting the SU(3) flavor breaking c_1^S and c_2^S terms. In the four quark picture of the scalar mesons, $E'_1 \equiv c_0'^S + c_1'^S - 2c_2'^S + c_3'^S$, $E'_2 \equiv c_0'^S - 2c_1'^S - 2c_2'^S + c_3'^S$, $E'_3 \equiv c_0'^S + c_1'^S + c_2'^S - 2c_3'^S$, $E'_4 \equiv c_0'^S + c_1'^S + c_2'^S + c_3'^S$, $E'_5 \equiv c_0'^S - 2c_1'^S + c_2'^S + c_3'^S$, $E'_1 = E'_2 = E'_3 = E'_4 = E'_5 = c_0'^S$ if neglecting the SU(3) flavor breaking $c_1'^S$, $c_2'^S$ and $c_3'^S$ terms.

Hadronic helicity amplitudes	ones for two-quark scenario	ones for four-quark scenario
$H(D^0 \rightarrow K_0^-\ell^+\nu_\ell)$	$E_1V_{cs}^*$	$E'_1V_{cs}^*$
$H(D^+ \rightarrow \bar{K}_0^0\ell^+\nu_\ell)$	$E_1V_{cs}^*$	$E'_1V_{cs}^*$
$H(D_s^+ \rightarrow f_0\ell^+\nu_\ell)$	$E_2V_{cs}^*$	$\sqrt{2}E'_2V_{cs}^*$
$H(D_s^+ \rightarrow f_0(980)\ell^+\nu_\ell)$	$\cos\theta_S E_2V_{cs}^*$	$\sqrt{2}\cos\phi_S E'_2V_{cs}^*$
$H(D_s^+ \rightarrow f_0(500)\ell^+\nu_\ell)$	$-\sin\theta_S E_2V_{cs}^*$	$-\sqrt{2}\sin\phi_S E'_2V_{cs}^*$
$H(D^0 \rightarrow a_0^-\ell^+\nu_\ell)$	$E_3V_{cd}^*$	$E'_3V_{cd}^*$
$H(D^+ \rightarrow a_0^0\ell^+\nu_\ell)$	$-\frac{1}{\sqrt{2}}E_3V_{cd}^*$	$-\frac{1}{\sqrt{2}}E'_3V_{cd}^*$
$H(D^+ \rightarrow f_0\ell^+\nu_\ell)$	0	$\frac{1}{\sqrt{2}}E'_3V_{cd}^*$
$H(D^+ \rightarrow \sigma\ell^+\nu_\ell)$	$\frac{1}{\sqrt{2}}E_3V_{cd}^*$	$E'_4V_{cd}^*$
$H(D^+ \rightarrow f_0(980)\ell^+\nu_\ell)$	$\frac{1}{\sqrt{2}}\sin\theta_S E_3V_{cd}^*$	$(\frac{1}{\sqrt{2}}E'_3\cos\phi_S + E'_4\sin\phi_S)V_{cd}^*$
$H(D^+ \rightarrow f_0(500)\ell^+\nu_\ell)$	$\frac{1}{\sqrt{2}}\cos\theta_S E_3V_{cd}^*$	$(-\frac{1}{\sqrt{2}}E'_3\sin\phi_S + E'_4\cos\phi_S)V_{cd}^*$
$H(D_s^+ \rightarrow K_0^0\ell^+\nu_\ell)$	$E_4V_{cd}^*$	$E'_5V_{cd}^*$

and two upper limits of $\mathcal{B}(D \rightarrow S\ell^+\nu_\ell, S \rightarrow P_1P_2)$ have been measured, and the data within 2σ errors are

$$\begin{aligned}
\mathcal{B}(D_s^+ \rightarrow f_0(980)e^+\nu_e, f_0(980) \rightarrow \pi^+\pi^-) &= (1.30 \pm 0.63) \times 10^{-3} \quad [81], \\
\mathcal{B}(D_s^+ \rightarrow f_0(980)e^+\nu_e, f_0(980) \rightarrow \pi^0\pi^0) &= (7.9 \pm 2.9) \times 10^{-4} \quad [82], \\
\mathcal{B}(D^0 \rightarrow a_0(980)^-e^+\nu_e, a_0(980)^- \rightarrow \eta\pi^-) &= (1.33_{-0.60}^{+0.68}) \times 10^{-4} \quad [1], \\
\mathcal{B}(D^+ \rightarrow a_0(980)^0e^+\nu_e, a_0(980)^0 \rightarrow \eta\pi^0) &= (1.7_{-1.4}^{+1.6}) \times 10^{-4} \quad [1], \\
\mathcal{B}(D^+ \rightarrow f_0(500)e^+\nu_e, f_0(500) \rightarrow \pi^+\pi^-) &= (6.3 \pm 1.0) \times 10^{-4} \quad [1], \\
\mathcal{B}(D^+ \rightarrow f_0(980)e^+\nu_e, f_0(980) \rightarrow \pi^+\pi^-) &< 2.8 \times 10^{-5} \quad [83], \\
\mathcal{B}(D_s^+ \rightarrow f_0(500)e^+\nu_e, f_0(500) \rightarrow \pi^0\pi^0) &< 6.4 \times 10^{-4} \quad [82].
\end{aligned} \tag{49}$$

Two cases S_1 and S_2 will be considered in the $D \rightarrow S\ell^+\nu_\ell$ decays. In S_1 case, only experimental datum of $\mathcal{B}(D_s^+ \rightarrow f_0(980)e^+\nu_e)$ is used to constrain one parameter c_0^S or $c_0'^S$ and then predict other not yet measured branching ratios. The numerical results of $\mathcal{B}(D \rightarrow S\ell^+\nu)$ in S_1 case are given in the 2-4th and 8th columns of Tab. IX. In the S_2 case, the experimental data of both $\mathcal{B}(D_s^+ \rightarrow f_0(980)e^+\nu_e)$ in Eq. (48) and $\mathcal{B}(D \rightarrow S\ell^+\nu_\ell, S \rightarrow P_1P_2)$ in Eq. (49) will be used to constrain the parameter c_0^S or $c_0'^S$. The predictions of $\mathcal{B}(D \rightarrow S\ell^+\nu)$ in S_2 case are listed in the 5-7th and 9th columns of Tab. IX. Our comments on the results in the $S_{1,2}$ cases are as follows.

- Results in the two quark picture:** In the two quark picture, the three possible ranges of the mixing angle, $25^\circ < \theta_S < 40^\circ$, $140^\circ < \theta_S < 165^\circ$ and $-30^\circ < \theta_S < 30^\circ$ [58, 68] have been analyzed. In S_1 case, using the data of $\mathcal{B}(D_s^+ \rightarrow f_0(980)e^+\nu_e)$, many predictions of $\mathcal{B}(D \rightarrow S\ell^+\nu)$ are obtained. As given in the 2-4th columns of Tab. IX, one can see that the predictions with $25^\circ < \theta_S < 40^\circ$ are similar to ones with $140^\circ < \theta_S < 165^\circ$, the predictions with $-30^\circ < \theta_S < 30^\circ$ are slightly different from the first two, and the errors of predictions are quite large. After adding the experimental bounds of $\mathcal{B}(D \rightarrow S\ell^+\nu_\ell, S \rightarrow P_1P_2)$, as given in the 5-7th columns of Tab. IX, the three possible ranges of the mixing angle θ_S are obviously constrained, and they reduce to $25^\circ < \theta_S < 35^\circ$, $144^\circ < \theta_S < 158^\circ$ and $22^\circ \leq |\theta_S| \leq 30^\circ$, respectively. In addition, the error of every prediction become smaller by adding the experimental bounds of $\mathcal{B}(D \rightarrow S\ell^+\nu_\ell, S \rightarrow P_1P_2)$.
- Results in the four quark picture:** The predictions in the four quark picture are listed in the 8-9th columns of Tab. IX. The majority of predictions in four quark picture are smaller than corresponding ones in two quark picture. Strong coupling constants g_4' and g_4 are appeared in $S \rightarrow P_1P_2$ decays with the four quark picture of light scalar mesons. At present, we only can determine $|\frac{g_4'}{g_4}|$ from the $S \rightarrow P_1P_2$ decays. The results of involved decays with both $\frac{g_4'}{g_4} > 0$ and $\frac{g_4'}{g_4} < 0$ are given in the 9th column of Tab. IX, and one can see that, except $\mathcal{B}(D_s^+ \rightarrow f_0(500)e^+\nu_e)$ and $\mathcal{B}(D_s^+ \rightarrow f_0(980)\mu^+\nu_\mu)$, the other involved branching ratios are not obviously affected by the choice of $\frac{g_4'}{g_4} > 0$ or $\frac{g_4'}{g_4} < 0$. The errors of the branching ratio predictions are obviously reduced by the experimental bounds of $\mathcal{B}(D \rightarrow S\ell^+\nu_\ell, S \rightarrow P_1P_2)$.
- Comparing with previous predictions:** Previous predictions are listed in the last column of Tab. IX. $\mathcal{B}(D_s^+ \rightarrow f_0(500)e^+\nu_e)$, $\mathcal{B}(D_s^+ \rightarrow f_0(500)\mu^+\nu_\mu)$ and $\mathcal{B}(D^+ \rightarrow f_0(500)\mu^+\nu_\mu)$ are predicted for the first time. Our predictions of $\mathcal{B}(D_s^+ \rightarrow f_0(980)\mu^+\nu_\mu)$, $\mathcal{B}(D^+ \rightarrow a_0^0e^+\nu_e)$, $\mathcal{B}(D^+ \rightarrow f_0(980)e^+\nu_e)$, $\mathcal{B}(D^+ \rightarrow f_0(500)e^+\nu_e)$ and $\mathcal{B}(D^+ \rightarrow a_0^0\mu^+\nu_\mu)$ are consistent with previous predictions in Refs. [78, 84, 85]. Our other predictions are about one order smaller or one order larger than previous ones in Refs. [67, 86].

TABLE IX: Branching ratios of $D \rightarrow S\ell^+\nu$ decays within 2σ errors. As given in Ref. [80], g'_4 and g_4 are strong coupling constants obtained by the SU(3) flavor symmetry in $S \rightarrow P_1 P_2$ decays, a denotes the results with $\frac{g'_4}{g_4} > 0$, and b denotes the results with two quark picture, and † denotes the results with four quark picture.

Branching ratios	ones for $2q$ state in S_1			ones for $2q$ state in S_2			ones for $4q$ state in S_1	ones for $4q$ state in S_2	Previous ones
	$[25^\circ, 40^\circ]$	$[140^\circ, 165^\circ]$	$[-30^\circ, 30^\circ]$	$[25^\circ, 35^\circ]$	$[144^\circ, 158^\circ]$	$22^\circ \leq \theta_S \leq 30^\circ$			
$\mathcal{B}(D^0 \rightarrow K_0^- e^+ \nu_e)(\times 10^{-3})$	3.38 ± 2.12	3.18 ± 2.05	2.57 ± 1.58	3.02 ± 1.11	3.00 ± 1.10	2.98 ± 1.05	1.11 ± 0.63	1.25 ± 0.45	$0.103 \pm 0.115^\dagger$ [67]
$\mathcal{B}(D^+ \rightarrow \bar{K}_0^0 e^+ \nu_e)(\times 10^{-3})$	8.66 ± 5.55	7.99 ± 5.02	7.02 ± 4.48	7.74 ± 2.88	7.78 ± 2.77	7.68 ± 2.78	2.85 ± 1.65	3.36 ± 1.25	$38.8 \pm 5.6^\dagger$ [67]
$\mathcal{B}(D_s^+ \rightarrow f_0(980)e^+ \nu_e)(\times 10^{-3})$	2.30 ± 0.80	2.30 ± 0.80	2.30 ± 0.80	2.58 ± 0.52	2.57 ± 0.53	2.71 ± 0.39	2.30 ± 0.80	2.49 ± 0.61^a 2.54 ± 0.56^b	$2.1 \pm 0.2^\dagger$ [78], $2^{+0.5^\dagger}_{-0.4}$ [84]
$\mathcal{B}(D_s^+ \rightarrow f_0(500)e^+ \nu_e)(\times 10^{-3})$	6.73 ± 6.11	5.98 ± 5.75	3.25 ± 3.25	1.49 ± 0.43	1.45 ± 0.46	1.42 ± 0.50	0.37 ± 0.37	0.31 ± 0.31^a 0.17 ± 0.17^b	
$\mathcal{B}(D^0 \rightarrow K_0^- \mu^+ \nu_\mu)(\times 10^{-3})$	2.90 ± 1.84	2.73 ± 1.77	2.20 ± 1.36	2.59 ± 0.97	2.57 ± 0.96	2.56 ± 0.92	0.95 ± 0.54	1.09 ± 0.39	$0.103 \pm 0.115^\dagger$ [67]
$\mathcal{B}(D^+ \rightarrow \bar{K}_0^0 \mu^+ \nu_\mu)(\times 10^{-3})$	7.46 ± 4.81	6.87 ± 4.33	6.04 ± 3.88	6.65 ± 2.52	6.69 ± 2.43	6.59 ± 2.43	2.45 ± 1.43	2.89 ± 1.09	$38.8 \pm 5.6^\dagger$ [67]
$\mathcal{B}(D_s^+ \rightarrow f_0(980)\mu^+ \nu_\mu)(\times 10^{-3})$	1.95 ± 0.70	1.95 ± 0.70	1.95 ± 0.69	2.20 ± 0.45	2.20 ± 0.45	2.32 ± 0.33	1.95 ± 0.70	2.12 ± 0.54^a 2.16 ± 0.49^b	$2.1 \pm 0.2^\dagger$ [78]
$\mathcal{B}(D_s^+ \rightarrow f_0(500)\mu^+ \nu_\mu)(\times 10^{-3})$	6.21 ± 5.66	5.53 ± 5.32	3.01 ± 3.01	1.33 ± 0.39	1.31 ± 0.43	1.28 ± 0.46	0.34 ± 0.34	0.29 ± 0.29^a 0.16 ± 0.16^b	
$\mathcal{B}(D^0 \rightarrow a_0^- e^+ \nu_e)(\times 10^{-5})$	9.99 ± 6.54	9.56 ± 6.50	8.34 ± 5.67	9.22 ± 3.98	9.09 ± 3.65	9.17 ± 3.58	3.42 ± 2.06	4.32 ± 1.17	$16.8 \pm 1.5^\dagger$ [78], $40.8^{+13.7^\dagger}_{-12.2}$ [86], $24.4 \pm 3.0^\dagger$ [67]
$\mathcal{B}(D^+ \rightarrow a_0^0 e^+ \nu_e)(\times 10^{-5})$	13.09 ± 8.62	12.62 ± 8.67	10.89 ± 7.35	12.09 ± 5.19	11.81 ± 4.71	11.97 ± 4.66	4.49 ± 2.71	5.68 ± 1.52	$21.8 \pm 3.8^\dagger$ [78], $54.0^{+17.8^\dagger}_{-15.9}$ [86] $6 \sim 8^\dagger$ [85], $5 \sim 5.4^\dagger$ [85]
$\mathcal{B}(D^+ \rightarrow f_0(980)e^+ \nu_e)(\times 10^{-5})$	3.92 ± 2.92	3.48 ± 3.13	1.59 ± 1.59	2.62 ± 0.82	2.52 ± 0.94	2.40 ± 0.80	3.14 ± 1.98	3.35 ± 1.80^a 3.89 ± 1.35^b	$7.78 \pm 0.68^\dagger$ [78], $5.7 \pm 1.3^\dagger$ [87] $0.4 \sim 3.5^\dagger$ [85], $1.9 \sim 6.3^\dagger$ [85]
$\mathcal{B}(D^+ \rightarrow f_0(500)e^+ \nu_e)(\times 10^{-4})$	4.05 ± 3.20	4.08 ± 3.10	4.21 ± 3.28	2.16 ± 0.96	2.59 ± 1.38	2.70 ± 1.28	4.97 ± 4.13	4.97 ± 3.34^a 4.95 ± 3.36^b	$0.4 \sim 0.6^\dagger$ [85], $0.88 \sim 1.4^\dagger$ [85]
$\mathcal{B}(D_s^+ \rightarrow K_0^0 e^+ \nu_e)(\times 10^{-4})$	3.73 ± 2.37	3.41 ± 2.13	2.99 ± 1.88	3.35 ± 1.21	3.32 ± 1.20	3.35 ± 1.15	1.25 ± 0.71	1.43 ± 0.51	$26.5 \pm 2.8^\dagger$ [67]
$\mathcal{B}(D^0 \rightarrow a_0^- \mu^+ \nu_\mu)(\times 10^{-5})$	8.25 ± 5.45	7.89 ± 5.42	6.91 ± 4.75	7.61 ± 3.37	7.51 ± 3.10	7.57 ± 3.04	2.83 ± 1.72	3.57 ± 0.99	$16.3 \pm 1.4^\dagger$ [78], $24.4 \pm 3.0^\dagger$ [67]
$\mathcal{B}(D^+ \rightarrow a_0^0 \mu^+ \nu_\mu)(\times 10^{-5})$	10.83 ± 7.19	10.44 ± 7.23	9.04 ± 6.16	10.00 ± 4.41	9.76 ± 4.00	9.89 ± 3.97	3.73 ± 2.28	4.69 ± 1.30	$21.2 \pm 3.7^\dagger$ [78]
$\mathcal{B}(D^+ \rightarrow f_0(980)\mu^+ \nu_\mu)(\times 10^{-5})$	3.23 ± 2.41	2.88 ± 2.60	1.32 ± 1.32	2.15 ± 0.70	2.09 ± 0.78	1.99 ± 0.66	2.56 ± 1.62	2.74 ± 1.49^a 3.20 ± 1.14^b	$7.87 \pm 0.67^\dagger$ [78]
$\mathcal{B}(D^+ \rightarrow f_0(500)\mu^+ \nu_\mu)(\times 10^{-4})$	3.69 ± 2.96	3.71 ± 2.86	3.84 ± 3.04	1.92 ± 0.88	2.32 ± 1.27	2.42 ± 1.19	4.54 ± 3.81	4.52 ± 3.10^a 4.49 ± 3.12^b	
$\mathcal{B}(D_s^+ \rightarrow K_0^0 \mu^+ \nu_\mu)(\times 10^{-4})$	3.28 ± 2.10	3.00 ± 1.88	2.62 ± 1.66	2.94 ± 1.08	2.91 ± 1.06	2.94 ± 1.02	1.10 ± 0.63	1.26 ± 0.45	$26.5 \pm 2.8^\dagger$ [67]

IV. Summary

Many semileptonic $D \rightarrow P/V/S\ell^+\nu_\ell$ decays have been measured, and these processes could be used to test the SU(3) flavor symmetry approach. In terms of the SU(3) flavor symmetry and the SU(3) flavor breaking, the amplitude relations have been obtained. Then using the present data of $\mathcal{B}(D \rightarrow P/V/S\ell^+\nu_\ell)$, we have presented a theoretical analysis of the $D \rightarrow P/V/S\ell^+\nu_\ell$ decays. Our main results can be summarized as follows.

- **$D \rightarrow P\ell^+\nu_\ell$ decays:** Our predictions with the SU(3) flavor symmetry in the C_1 case and the predictions after adding SU(3) flavor breaking contributions in the C_4 case are quite consistent with all present experimental data of $\mathcal{B}(D \rightarrow P\ell^+\nu_\ell)$ within 2σ errors. In the C_2 and C_3 cases, our SU(3) flavor symmetry predictions are consistent with all present experimental data except $\mathcal{B}(D^+ \rightarrow \pi^0\ell^+\nu_\ell)$ and $\mathcal{B}(D^0 \rightarrow \pi^-\ell^+\nu_\ell)$, which are slight larger than their experiential upper limits. The not yet measured $\mathcal{B}(D_s^+ \rightarrow \pi^0e^+\nu_e)$, $\mathcal{B}(D^+ \rightarrow \eta'\mu^+\nu_\mu)$, $\mathcal{B}(D_s^+ \rightarrow K^0\mu^+\nu_\mu)$, $\mathcal{B}(D_s^+ \rightarrow \pi^0\mu^+\nu_\mu)$, $\mathcal{B}(D_s^+ \rightarrow \pi^0\tau^+\nu_\tau)$ and the lepton flavor universality parameters have been obtained. Moreover, the forward-backward asymmetries, the lepton-side convexity parameters, the longitudinal (transverse) polarizations of the final charged leptons with two ways of integration for the $D \rightarrow P\ell^+\nu_\ell$ decays have been predicted. The q^2 dependence of corresponding differential quantities of the $D \rightarrow P\ell^+\nu_\ell$ decays in the C_3 case have been displayed.
- **$D \rightarrow V\ell^+\nu_\ell$ decays:** As given in the C_1 , C_2 and C_3 cases, our SU(3) flavor symmetry predictions of $\mathcal{B}(D^+ \rightarrow \omega e^+\nu_e)$ and $\mathcal{B}(D^0 \rightarrow \rho^-\mu^+\nu_\mu)$ are slightly larger than its experimental upper limits, and other SU(3) flavor symmetry predictions are consistent with present data. After considering the SU(3) flavor breaking effects, as given in the C_4 case, all predictions are consistent with present data. The not yet measured or not yet well measured branching ratios of $D^+ \rightarrow \phi e^+\nu_e$, $D_s^+ \rightarrow \omega e^+\nu_e$, $D^+ \rightarrow \phi\mu^+\nu_\mu$, $D_s^+ \rightarrow \omega\mu^+\nu_\mu$, and $D_s^+ \rightarrow K^{*0}\mu^+\nu_\mu$ have been predicted. The q^2 dependence of corresponding differential quantities of the $D \rightarrow V\ell^+\nu_\ell$ decays in the C_3 case have also been displayed.
- **$D \rightarrow S\ell^+\nu_\ell$ decays:** Among 18 $D \rightarrow S\ell^+\nu_\ell$ decay modes, only $\mathcal{B}(D_s^+ \rightarrow f_0(980)e^+\nu_e)$ has been measured, and this experimental datum has been used to constrain the SU(3) flavor symmetry parameter and then predict other not yet measured branching ratios. Furthermore, the relevant experimental bounds of $\mathcal{B}(D \rightarrow S\ell^+\nu_\ell)$, $S \rightarrow P_1P_2$ have also been added. The two quark and the four quark scenarios for the light scalar mesons are considered, and the three possible ranges of the mixing angle θ_S in the two quark picture have been analyzed.

The SU(3) flavor symmetry is approximate approach, and it can still provide very useful information. We have found that the SU(3) flavor symmetry approach works well in the semileptonic $D \rightarrow P/V\ell^+\nu_\ell$ decays, and the SU(3) flavor symmetry predictions of the $D \rightarrow S\ell^+\nu_\ell$ decays need to be further tested, and our predictions of the $D \rightarrow S\ell^+\nu_\ell$ decays are useful for probing the structure of light scalar mesons. According to our predictions, some decay modes could be observed at BESIII, LHCb or BelleII in near future experiments.

ACKNOWLEDGEMENTS

The work was supported by the National Natural Science Foundation of China (12175088).

References

- [1] R. L. Workman et al. (Particle Data Group), Prog. Theor. Exp. Phys. **2022**, 083C01 (2022).
- [2] D. Melikhov and B. Stech, Phys. Rev. D **62** (2000), 014006 [arXiv:hep-ph/0001113 [hep-ph]].
- [3] H. Y. Cheng and X. W. Kang, Eur. Phys. J. C **77** (2017) no.9, 587 [erratum: Eur. Phys. J. C **77** (2017) no.12, 863] [arXiv:1707.02851 [hep-ph]].
- [4] N. R. Soni, M. A. Ivanov, J. G. Körner, J. N. Pandya, P. Santorelli and C. T. Tran, Phys. Rev. D **98** (2018) no.11, 114031 [arXiv:1810.11907 [hep-ph]].
- [5] Q. Chang, X. N. Li, X. Q. Li, F. Su and Y. D. Yang, Phys. Rev. D **98** (2018) no.11, 114018 [arXiv:1810.00296 [hep-ph]].
- [6] Q. Chang, X. L. Wang and L. T. Wang, Chin. Phys. C **44** (2020) no.8, 083105 [arXiv:2003.10833 [hep-ph]].
- [7] R. N. Faustov, V. O. Galkin and X. W. Kang, Phys. Rev. D **101** (2020) no.1, 013004 [arXiv:1911.08209 [hep-ph]].
- [8] P. Ball, Phys. Rev. D **48** (1993), 3190-3203 [arXiv:hep-ph/9305267 [hep-ph]].
- [9] S. Bhattacharyya, M. Haiduc, A. Tania Neagu and E. Fîru, Eur. Phys. J. Plus **134** (2019) no.1, 37 [arXiv:1709.00882 [nucl-ex]].
- [10] H. B. Fu, L. Zeng, R. Lü, W. Cheng and X. G. Wu, Eur. Phys. J. C **80** (2020) no.3, 194 [arXiv:1808.06412 [hep-ph]].
- [11] H. B. Fu, W. Cheng, L. Zeng, D. D. Hu and T. Zhong, Phys. Rev. Res. **2** (2020) no.4, 043129 [arXiv:2003.07626 [hep-ph]].
- [12] I. L. Grach, I. M. Narodetsky and S. Simula, Phys. Lett. B **385** (1996), 317-323 [arXiv:hep-ph/9605349 [hep-ph]].
- [13] H. Y. Cheng, C. K. Chua and C. W. Hwang, Phys. Rev. D **69** (2004), 074025 [arXiv:hep-ph/0310359 [hep-ph]].
- [14] Q. Chang, X. N. Li and L. T. Wang, Eur. Phys. J. C **79** (2019) no.5, 422 [arXiv:1905.05098 [hep-ph]].
- [15] V. Lubicz *et al.* [ETM], Phys. Rev. D **98** (2018) no.1, 014516 [arXiv:1803.04807 [hep-lat]].
- [16] V. Lubicz *et al.* [ETM], Phys. Rev. D **96** (2017) no.5, 054514 [erratum: Phys. Rev. D **99** (2019) no.9, 099902; erratum: Phys. Rev. D **100** (2019) no.7, 079901] [arXiv:1706.03017 [hep-lat]].
- [17] X. G. He, Eur. Phys. J. C **9**, 443 (1999) [hep-ph/9810397].
- [18] X. G. He, Y. K. Hsiao, J. Q. Shi, Y. L. Wu and Y. F. Zhou, Phys. Rev. D **64**, 034002 (2001) [hep-ph/0011337].
- [19] H. K. Fu, X. G. He and Y. K. Hsiao, Phys. Rev. D **69**, 074002 (2004) [hep-ph/0304242].
- [20] Y. K. Hsiao, C. F. Chang and X. G. He, Phys. Rev. D **93**, no. 11, 114002 (2016) [arXiv:1512.09223 [hep-ph]].
- [21] X. G. He and G. N. Li, Phys. Lett. B **750**, 82 (2015) [arXiv:1501.00646 [hep-ph]].
- [22] M. Gronau, O. F. Hernandez, D. London and J. L. Rosner, Phys. Rev. D **50**, 4529 (1994) [hep-ph/9404283].
- [23] M. Gronau, O. F. Hernandez, D. London and J. L. Rosner, Phys. Rev. D **52**, 6356 (1995) [hep-ph/9504326].
- [24] S. H. Zhou, Q. A. Zhang, W. R. Lyu and C. D. Lü, Eur. Phys. J. C **77**, no. 2, 125 (2017) [arXiv:1608.02819 [hep-ph]].
- [25] H. Y. Cheng, C. W. Chiang and A. L. Kuo, Phys. Rev. D **91**, no. 1, 014011 (2015) [arXiv:1409.5026 [hep-ph]].
- [26] M. He, X. G. He and G. N. Li, Phys. Rev. D **92**, no. 3, 036010 (2015) [arXiv:1507.07990 [hep-ph]].
- [27] N. G. Deshpande and X. G. He, Phys. Rev. Lett. **75**, 1703 (1995) [hep-ph/9412393].
- [28] S. Shivashankara, W. Wu and A. Datta, Phys. Rev. D **91**, 115003 (2015) [arXiv:1502.07230 [hep-ph]].
- [29] R. M. Wang, Y. G. Xu, C. Hua and X. D. Cheng, Phys. Rev. D **103** (2021) no.1, 013007 [arXiv:2101.02421 [hep-ph]].
- [30] R. M. Wang, X. D. Cheng, Y. Y. Fan, J. L. Zhang and Y. G. Xu, J. Phys. G **48** (2021) no.8, 085001 [arXiv:2008.06624 [hep-ph]].
- [31] Y. Grossman and D. J. Robinson, JHEP **1304**, 067 (2013) [arXiv:1211.3361 [hep-ph]].
- [32] D. Pirtskhalava and P. Uttayarat, Phys. Lett. B **712**, 81 (2012) [arXiv:1112.5451 [hep-ph]].
- [33] H. Y. Cheng and C. W. Chiang, Phys. Rev. D **86**, 014014 (2012) [arXiv:1205.0580 [hep-ph]].

- [34] M. J. Savage and R. P. Springer, Phys. Rev. D **42**, 1527 (1990).
- [35] M. J. Savage, Phys. Lett. B **257**, 414 (1991).
- [36] G. Altarelli, N. Cabibbo and L. Maiani, Phys. Lett. **57B**, 277 (1975).
- [37] C. D. Lü, W. Wang and F. S. Yu, Phys. Rev. D **93**, no. 5, 056008 (2016) [arXiv:1601.04241 [hep-ph]].
- [38] C. Q. Geng, Y. K. Hsiao, Y. H. Lin and L. L. Liu, Phys. Lett. B **776**, 265 (2018) [arXiv:1708.02460 [hep-ph]].
- [39] C. Q. Geng, Y. K. Hsiao, C. W. Liu and T. H. Tsai, Phys. Rev. D **97**, no. 7, 073006 (2018) [arXiv:1801.03276 [hep-ph]].
- [40] C. Q. Geng, Y. K. Hsiao, C. W. Liu and T. H. Tsai, JHEP **1711**, 147 (2017) [arXiv:1709.00808 [hep-ph]].
- [41] C. Q. Geng, C. W. Liu, T. H. Tsai and S. W. Yeh, arXiv:1901.05610 [hep-ph].
- [42] W. Wang, Z. P. Xing and J. Xu, Eur. Phys. J. C **77**, no. 11, 800 (2017) [arXiv:1707.06570 [hep-ph]].
- [43] D. Wang, arXiv:1901.01776 [hep-ph].
- [44] D. Wang, P. F. Guo, W. H. Long and F. S. Yu, JHEP **1803**, 066 (2018) [arXiv:1709.09873 [hep-ph]].
- [45] S. Müller, U. Nierste and S. Schacht, Phys. Rev. D **92**, no. 1, 014004 (2015) [arXiv:1503.06759 [hep-ph]].
- [46] J. Barranco, D. Delepine, V. Gonzalez Macias and L. Lopez-Lozano, arXiv:1404.0454 [hep-ph].
- [47] J. Barranco, D. Delepine, V. Gonzalez Macias and L. Lopez-Lozano, Phys. Lett. B **731**, 36 (2014) [arXiv:1303.3896 [hep-ph]].
- [48] A. G. Akeroyd and F. Mahmoudi, JHEP **0904**, 121 (2009) [arXiv:0902.2393 [hep-ph]].
- [49] B. A. Dobrescu and A. S. Kronfeld, Phys. Rev. Lett. **100**, 241802 (2008) [arXiv:0803.0512 [hep-ph]].
- [50] A. G. Akeroyd and C. H. Chen, Phys. Rev. D **75**, 075004 (2007) [hep-ph/0701078].
- [51] S. Fajfer and J. F. Kamenik, Phys. Rev. D **73**, 057503 (2006) [hep-ph/0601028].
- [52] S. Fajfer and J. F. Kamenik, Phys. Rev. D **72**, 034029 (2005) [hep-ph/0506051].
- [53] S. Fajfer and J. F. Kamenik, Phys. Rev. D **71**, 014020 (2005) [hep-ph/0412140].
- [54] A. G. Akeroyd, Prog. Theor. Phys. **111**, 295 (2004) [hep-ph/0308260].
- [55] A. G. Akeroyd and S. Recksiegel, Phys. Lett. B **554**, 38 (2003) [hep-ph/0210376].
- [56] M. A. Ivanov, J. G. Körner, J. N. Pandya, P. Santorelli, N. R. Soni and C. T. Tran, Front. Phys. (Beijing) **14** (2019) no.6, 64401 [arXiv:1904.07740 [hep-ph]].
- [57] X. G. He, Y. J. Shi and W. Wang, Eur. Phys. J. C **80**, no.5, 359 (2020) [arXiv:1811.03480 [hep-ph]].
- [58] H. Y. Cheng, C. K. Chua and K. C. Yang, Phys. Rev. D **73** (2006), 014017 [arXiv:hep-ph/0508104 [hep-ph]].
- [59] L. Maiani, F. Piccinini, A. D. Polosa and V. Riquer, Phys. Rev. Lett. **93** (2004), 212002 [arXiv:hep-ph/0407017 [hep-ph]].
- [60] L. Y. Dai, X. W. Kang and U. G. Meißner, Phys. Rev. D **98** (2018) no.7, 074033 [arXiv:1808.05057 [hep-ph]].
- [61] G. 't Hooft, G. Isidori, L. Maiani, A. D. Polosa and V. Riquer, Phys. Lett. B **662** (2008), 424-430 [arXiv:0801.2288 [hep-ph]].
- [62] J. R. Pelaez, Phys. Rev. Lett. **92** (2004), 102001 [arXiv:hep-ph/0309292 [hep-ph]].
- [63] Y. J. Sun, Z. H. Li and T. Huang, Phys. Rev. D **83** (2011), 025024 [arXiv:1011.3901 [hep-ph]].
- [64] J. A. Oller and E. Oset, Nucl. Phys. A **620** (1997), 438-456 [erratum: Nucl. Phys. A **652** (1999), 407-409] [arXiv:hep-ph/9702314 [hep-ph]].
- [65] V. Baru, J. Haidenbauer, C. Hanhart, Y. Kalashnikova and A. E. Kudryavtsev, Phys. Lett. B **586** (2004), 53-61 [arXiv:hep-ph/0308129 [hep-ph]].
- [66] N. N. Achasov, V. V. Gubin and V. I. Shevchenko, Phys. Rev. D **56** (1997), 203-211 [arXiv:hep-ph/9605245 [hep-ph]].
- [67] S. Momeni and M. Saghebfar, Eur. Phys. J. C **82** (2022) no.5, 473
- [68] R. Aaij *et al.* [LHCb], Phys. Rev. D **87** (2013) no.5, 052001 [arXiv:1301.5347 [hep-ex]].
- [69] R. L. Jaffe, Phys. Rev. D **15** (1977), 267
- [70] D. Xu, G. N. Li and X. G. He, Int. J. Mod. Phys. A **29** (2014), 1450011 [arXiv:1307.7186 [hep-ph]].
- [71] M. Tanaka and R. Watanabe, Phys. Rev. D **82**, 034027 (2010) [arXiv:1005.4306 [hep-ph]].

- [72] M. Tanaka, Z. Phys. C **67**, 321 (1995) [hep-ph/9411405].
- [73] S. Fajfer, J. F. Kamenik and I. Nisandzic, Phys. Rev. D **85**, 094025 (2012) [arXiv:1203.2654 [hep-ph]].
- [74] A. Celis, M. Jung, X. Q. Li and A. Pich, JHEP **1301**, 054 (2013) [arXiv:1210.8443 [hep-ph]].
- [75] C. Bobeth, G. Hiller and D. van Dyk, JHEP **1007**, 098 (2010) [arXiv:1006.5013 [hep-ph]].
- [76] H. B. Li and M. Z. Yang, Phys. Lett. B **811** (2020), 135879 [arXiv:2006.15798 [hep-ph]].
- [77] N. N. Achasov and A. V. Kiselev, Phys. Rev. D **86** (2012), 114010 [arXiv:1206.5500 [hep-ph]].
- [78] N. R. Soni, A. N. Gadaria, J. J. Patel and J. N. Pandya, Phys. Rev. D **102** (2020) no.1, 016013 [arXiv:2001.10195 [hep-ph]].
- [79] X. Leng, X. L. Mu, Z. T. Zou and Y. Li, Chin. Phys. C **45** (2021) no.6, 063107 [arXiv:2011.01061 [hep-ph]].
- [80] Ru-Min Wang, Yi-Jie Zhang, Yi Qiao, Xiao-Dong Cheng and Yuan-Guo Xu, Four-body Semileptonic Charm Decays $D \rightarrow P_1 P_2 \ell^+ \nu_\ell$ with the SU(3) Flavor Symmetry, in preparation.
- [81] J. Hietala, D. Cronin-Hennessy, T. Pedlar and I. Shipsey, Phys. Rev. D **92** (2015) no.1, 012009 [arXiv:1505.04205 [hep-ex]].
- [82] M. Ablikim *et al.* [BESIII], [arXiv:2110.13994 [hep-ex]].
- [83] M. Ablikim *et al.* [BESIII], Phys. Rev. Lett. **122** (2019) no.6, 062001 [arXiv:1809.06496 [hep-ex]].
- [84] P. Colangelo, F. De Fazio and W. Wang, Phys. Rev. D **81** (2010), 074001 [arXiv:1002.2880 [hep-ph]].
- [85] W. Wang and C. D. Lü, Phys. Rev. D **82** (2010), 034016 [arXiv:0910.0613 [hep-ph]].
- [86] X. D. Cheng, H. B. Li, B. Wei, Y. G. Xu and M. Z. Yang, Phys. Rev. D **96** (2017) no.3, 033002 [arXiv:1706.01019 [hep-ph]].
- [87] H. W. Ke, X. Q. Li and Z. T. Wei, Phys. Rev. D **80** (2009), 074030 [arXiv:0907.5465 [hep-ph]].